

Update to the JEF proposal (PR12-14-004)

H. Al Ghouli, B. E. Cannon, V. Crede, A. Ernst, P. Eugenio, A. I. Ostrovidov, and A. Tsaris

Florida State University, Tallahassee, Florida 32306, USA

A. Ali, R. Dzhygadlo, K. Goetzen, A. Hamdi,

F. Nerling, K. J. Peters, C. Schwarz, and J. Schwiening

GSI Helmholtzzentrum für Schwerionenforschung GmbH, D-64291 Darmstadt, Germany

E. G. Anassontzis, C. Kourkouveli, and G. Vasileiadis

National and Kapodistrian University of Athens, 15771 Athens, Greece

A. Austregesilo, F. Barbosa, T. Britton, E. Chudakov, M. M. Dalton, A. Deur,

H. Egiyan, S. Furletov, M. M. Ito, D. Lawrence, D. Mack, P. T. Mattione,

M. McCaughan, L. Pentchev, E. Pooser, E. S. Smith, A. Somov (co-spokesperson),

S. Taylor (co-spokesperson), T. Whitlatch, B. Zihlmann, and J. Benesch*

Thomas Jefferson National Accelerator Facility,

Newport News, Virginia 23606, USA

A. Barnes, R. T. Jones, J. McIntyre, F. Mokaya, and B. Pratt

University of Connecticut, Storrs, Connecticut 06269, USA

T. D. Beattie, A. M. Foda, G. M. Huber, G. J. Lolos, Z. Papandreou

(co-spokesperson), A. Yu. Semenov, I. A. Semenova, and A. Teymurazyan

University of Regina, Regina, Saskatchewan, Canada S4S 0A2

V. V. Berdnikov, D. Romanov, and S. Somov

National Research Nuclear University Moscow

Engineering Physics Institute, Moscow 115409, Russia

T. Black and L. Gan (spokesperson)

University of North Carolina at Wilmington,

Wilmington, North Carolina 28403, USA

W. Boeglin, L. Guo, M. Kamel, W. Phelps, and J. Reinhold

Florida International University, Miami, Florida 33199, USA

W. J. Briscoe, F. J. Klein, and I. I. Strakovsky

The George Washington University, Washington, D.C. 20052, USA

W. K. Brooks, H. Hakobyan, S. Kuleshov, and O. Soto

Universidad Técnica Federico Santa María, Casilla 110-V Valparaíso, Chile

S. Dobbs, L. Robison, K. K. Seth, A. Tomaradze, and T. Xiao

Northwestern University, Evanston, Illinois 60208, USA

A. Dolgolenko, V. S. Goryachev, I. Larin, V. Matveev, and V. Tarasov

Institute for Theoretical and Experimental Physics, Moscow 117259, Russia

M. Dugger, B. G. Ritchie, and N. Sparks

Arizona State University, Tempe, Arizona 85287, USA

C. Fanelli, J. Hardin, M. Patsyuk, M. Williams, and Y. Yang

Massachusetts Institute of Technology,

Cambridge, Massachusetts 02139, USA

J. Frye, R. E. Mitchell, M. R. Shepherd, A. Subedi, and J. Zarling

Indiana University, Bloomington, Indiana 47405, USA

A. Gasparian, M. Levillain, and R. Pedroni

North Carolina A&T State University,

Greensboro, North Carolina 27411, USA

V. Gauzshtein, I. Kuznetsov, and V. Lyubovitskij

Tomsk State University, 634050 Tomsk, Russia and

Tomsk Polytechnic University, 634050 Tomsk, Russia

N. Gevorgyan, V. Kakoyan, and H. Marukyan

A. I. Alikhanian National Science Laboratory

(Yerevan Physics Institute), 0036 Yerevan, Armenia

S. Han, N. Qin, Z. Zhang, and X. Zhou

Wuhan University, Wuhan, Hubei 430072, People's Republic of China

D. G. Ireland, K. Livingston, P. Pauli, and D. Werthmüller

University of Glasgow, Glasgow G12 8QQ, United Kingdom

N. S. Jarvis, W. I. Levine, M. McCracken, W. McGinley,

C. A. Meyer, R. A. Schumacher, and M. J. Staib

Carnegie Mellon University, Pittsburgh, Pennsylvania 15213, USA

G. Kalicy and D. I. Sober

Catholic University of America, Washington, D.C. 20064, USA

R. Miskimen, B. Holstein[†], and M. Ramsey-Musolf[†]

University of Massachusetts, Amherst, Massachusetts 01003, USA

C. Salgado

Norfolk State University, Norfolk, Virginia 23504, USA

J. R. Stevens, D. Armstrong*, and W. Deconinck*

College of William and Mary, Williamsburg, Virginia 23185, USA

P. King* and J. Roche*

Ohio University, Athens, OH, USA

L. Roca*

Universidad de Murcia, E-30071 Murcia, Spain

K. E. Mesick*

Los Alamos National Laboratory (LANL), Los Alamos, NM 87545, USA

N. Simicevic* and S. Wells*

Louisiana Tech University, Ruston, LA, USA

J. Dunne* and D. Dutta*

Mississippi State University, Mississippi State, MS, USA

S. Gevorkyan*

Joint Institute for Nuclear Research, Dubna, Russia

D. Chen*, X. Chen*, J. He*, R. Wang*, H. Yang*, and P. Zhang*

Institute of Modern Physics, Lanzhou, People's Republic of China

S. Fang* and H. Lui*

Institute of High Energy Physics, Beijing, People's Republic of China

X. Z. Bai*, J. Feng*, H. X. He*, S. Y. Hu*, S. Y. Jian*, X. M. Li*,

C. Shan*, H. H. Xia*, L. Ye*, J. Yuan*, J. Zhou*, and S. H. Zhou*

Chinese Institute of Atomic Energy, Beijing, People's Republic of China

B. Hu*, L. Ma*, and Y. Zhang*

Lanzhou University, Lanzhou, People's Republic of China

S. Barkanova[†]

Acadia University, Wolfville, Nova Scotia, Canada

G. Colangelo[†]

University of Bern, Sidlerstrasse 5, CH3012, Switzerland

B. Kubis[†]

University of Bonn, D-53115 Bonn, Germany

B. Martemyanov[†]

Moscow Institute for Theoretical and Experimental Physics (ITEP), Moscow, Russia

E. Passemar[†]

Thomas Jefferson National Accelerator Facility and Indiana University,

Bloomington, Indiana 47405, USA and Indiana University – Center

for Exploration of Energy and Matter, Bloomington, IN 47408, USA

J. Bijnens[†]

Lund University, SE 223-62 Lund, Sweden

A. Aleksejevs[†]

Memorial University, Grenfell Campus, Canada

S. Tulin[†]

York University, Toronto, Ontario, M3J 1P3, Canada

J. Goity[†]

*Thomas Jefferson National Accelerator Facility and Hampton University,
Newport News, Virginia 23606, USA*

(Dated: May 22, 2017)

(The GLUEX Collaboration and other participants (*Non-GlueX, [†]Theory advisor))

Contents

I. Executive summary	8
II. Introduction	9
III. Motivation for sub-GeV dark gauge boson	12
IV. Recent experimental developments for leptophobic B' search	15
V. Unique Features of JEF Experiment in η Decays	16
VI. Extension to η' physics	20
VII. Hybrid Calorimeter FCAL-II	22
A. Update on FCAL-II, cost, and manpower	23
B. Impact of FCAL-II Installation on the Run Schedule in Hall D	26
VIII. Simulation of the $\eta \rightarrow \pi^0 \gamma \gamma$ signal	27
IX. Background simulations	29
X. Rates under the GlueX-IV running configuration	36
A. Tagger coincidental rates	36
B. Numbers of the tagged η and η'	38
XI. Beam Time	39
XII. Summary	40

References 40

A. Alternate $2\pi^0$ model 43

I. EXECUTIVE SUMMARY

This document is an update to the conditionally-approved Jlab Eta Factory (JEF) Experiment PR12-14-004 [1] intended to address issues raised by the PAC “that FCAL-II and the associated JEF physics program be fully incorporated to run in parallel with GlueX”. We performed detailed simulations of our key signal channel $\eta \rightarrow \pi^0 \gamma \gamma$ along with various background channels under the GlueX Phase-IV [2] running conditions. These studies clearly suggest that the JEF experiment has full capability to take data concurrently with GlueX or any other experiments using a LH₂ target in Hall D, while the experimental sensitivity to the key physics goal will remain the same or even improve relative to what was stated in the original proposal due to potential for more beam time. The projected FCAL-II installation will have minimal impact on the run schedule and will offer a state-of-art, high resolution, high granularity, and radiation-resistant calorimeter for all approved (and future) experiments in Hall D.

The JEF program aims to perform precision measurements of various η decays with emphasis on rare neutral modes. Since the production rates of η and η' are similar under the JEF experimental conditions, the same data set will offer sensitive probes for η' decays as well. Compared to all existing and planned η/η' experiments in the world, the unique feature of the JEF program is to offer a clean data set in the rare neutral decays of η and η' with up to two orders of magnitude reduction in the backgrounds. The JEF data will offer significant different systematics compared to the other $\eta^{(\prime)}$ programs.

The η meson, with quantum numbers of the vacuum, provides a unique, flavor-conserving laboratory to probe the isospin-violating sector of low energy QCD and search for physics beyond the Standard Model. The measurement of $\eta \rightarrow 3\pi$ has been in progress by running in parallel to the GlueX experiment to improve our understanding of the light quark mass ratio. For phase II our priority physics campaigns are centered around neutral rare decays of the η with following key signal channels:

- A search for a leptophobic dark boson B' coupled to baryon number is complementary to ongoing searches for a dark photon or invisible decay searches for dark sector particles. For 100 days of beam time, a search for B' in the mass range 0.14-0.54

GeV through $\eta \rightarrow \gamma + B'(\rightarrow \gamma + \pi^0)$ will improve existing bounds by two orders of magnitude, with sensitivity to the baryonic fine structure constant α_B as low as 10^{-7} . Further extension to $\eta' \rightarrow \gamma + B'(\rightarrow \pi^+\pi^-\pi^0)$ and peak hunting in $\pi^0\gamma$ and $\pi^+\pi^-\pi^0$ spectra for direct B' photoproduction will broaden the mass coverage up to 1 GeV.

- A low-background measurement of the rare decay $\eta \rightarrow \pi^0\gamma\gamma$ provides a clean, rare window into $\mathcal{O}(p^6)$ in Chiral Perturbation Theory (ChPT). With sufficient precision in the Dalitz distribution, for the first time we will be able to determine two $\mathcal{O}(p^6)$ Low Energy Constants in a model-independent way and to explore the role of scalar meson dynamics in ChPT.
- A search for the SM forbidden decay $\eta \rightarrow 3\gamma$ (as well as $\eta \rightarrow 2\pi^0\gamma$ and $\eta \rightarrow 3\pi^0\gamma$) will lead to the best direct constraints on new C violating, P conserving reactions, which is a largely unexplored area of fundamental symmetry tests [3].

II. INTRODUCTION

The Standard Model (SM) is successful in describing a wide range of phenomena in nuclear and particle physics. Its success has been crowned with the discovery of the Higgs boson at CERN in 2012, the last missing fundamental particle in the SM. However, there are strong indications that the SM is incomplete. The theory needs 19 input parameters and does not explain the origin of the three fermion families, nor why their masses are widely different. Furthermore, the SM fails to explain the dominance of matter over anti-matter in the universe or the dark matter relic density. Extending the SM to resolve these questions is a high priority.

Another high priority is to better understand the rich complexity of confinement QCD. For example, can we confirm predictions for low energy phenomenology such as the meson spectrum with explicit gluonic degrees of freedom, or correct for strong re-scattering well enough to accurately determine basic SM parameters like $m_u - m_d$? A promising theoretical framework that can be used to address these challenging but interesting questions is Chiral Perturbation Theory (ChPT), which is based on the chiral symmetry of QCD in the massless quark limit. Tests of ChPT predictions and understanding its links to the underlying QCD

are important.

Decays of the neutral and long-lived η meson provide a unique, flavor-conserving laboratory to probe the isospin violating sector of low energy QCD and search for physics beyond the SM. Spontaneously broken chiral symmetry in QCD gives birth to the η as one of the Goldstone Bosons. The η is an eigenstate of P, C, CP, and G ($I^G J^{PC} = 0^+0^{-+}$) whose strong and electromagnetic decays are either anomalous or forbidden to the lowest order due to P, C, CP, G-parity and angular momentum conservation [5]. This enhances the relative importance of higher order contributions, making η decays a sensitive hadronic probe for searching for rare processes or testing discrete symmetries.

We propose to test low-energy QCD and search for new physics Beyond Standard Model (BSM) in η decays using the high energy photon tagging facility and the GlueX detector in Hall D. Table I summarizes various η decays in the scope of this proposal. Data for the SM-allowed decay channels have been accumulating in the nominal GlueX data stream since 2015. The proposed upgraded Forward Calorimeter (FCAL-II) will afford the improvement of limits by 1–2 orders of magnitude for other rare or SM-forbidden channels leading to all-neutral final states.

In 2014, we submitted an earlier version of this present proposal with the title “Eta Decays with Emphasis on Rare Neutral Modes: The JLab Eta Factory (JEF) Experiment” (PR12-14-004) [1] with the following main physics goals: (i) a search for a leptophobic dark gauge boson coupling to baryon number with a mass between m_{π^0} and m_η to improve the existing bounds on the baryonic fine structure constant α_B by two orders of magnitude; (ii) a search for the C-violating and P-conserving η decays with an order of magnitude improvement over current branching ratio upper limits; (iii) a determination of two low energy constants entering chiral perturbation theory at $\mathcal{O}(p^6)$ from the $\eta \rightarrow \pi^0\gamma\gamma$ decay, and with sufficient precision in the Dalitz distribution to explore the role of scalar meson dynamics in this channel for the first time; and (iv) a clean determination of the light quark mass ratio $\mathcal{Q} \equiv (m_s^2 - \hat{m}^2)/(m_d^2 - m_u^2)$ with $\hat{m} \equiv (m_u + m_d)/2$ from $\eta \rightarrow 3\pi$ decays. The original proposal was conditionally approved by PAC42 with following recommendations:

“The PAC understands the very strong scientific interest of performing new mea-

Mode	Branching Ratio	Physics Highlight	Photons
priority:			
$\gamma + B'$	beyond SM	leptophobic dark boson	4
$\pi^0 2\gamma$	$(2.7 \pm 0.5) \times 10^{-4}$	χ PTh at $\mathcal{O}(p^6)$	4
$3\pi^0$	$(32.7 \pm 0.2)\%$	$m_u - m_d$	6
$\pi^+ \pi^- \pi^0$	$(22.9 \pm 0.3)\%$	$m_u - m_d$, CV	2
3γ	$< 1.6 \times 10^{-5}$	CV, CPV	3
ancillary:			
4γ	$< 2.8 \times 10^{-4}$	$< 10^{-11}$ [6]	4
$2\pi^0$	$< 3.5 \times 10^{-4}$	CPV, PV	4
$2\pi^0 \gamma$	$< 5 \times 10^{-4}$	CV, CPV	5
$3\pi^0 \gamma$	$< 6 \times 10^{-5}$	CV, CPV	7
$4\pi^0$	$< 6.9 \times 10^{-7}$	CPV, PV	8
$\pi^0 \gamma$	$< 9 \times 10^{-5}$	CV, Ang. Mom. viol.	3
normalization:			
2γ	$(39.4 \pm 0.2)\%$	anomaly, η - η' mixing E12-10-011	2

TABLE I: The η decays highlighted in this proposal, plus related ancillary channels [68]. The $\eta \rightarrow 2\gamma$ will be measured in an approved Primakoff experiment (E12-10-011) that is currently under preparation in Hall D.

surements of rare η decays with improved sensitivity to test the SM. In particular, the PAC sees the determination (iv) of \mathcal{Q} from the $\eta \rightarrow 3\pi$ decay ratio and the Dalitz distribution as the most compelling physics result and recommends to perform this measurement as a run group with GlueX and experiment PR12-10-011 (which is approved to measure the $\eta \rightarrow 2\gamma$ decay width via the Primakoff effect). This part of the proposal can be performed with the existing calorimeter (FCAL) used by GlueX. The other three physics goals (i)-(iii) will need the FCAL-II, which will mean a major investment in various kinds of resources. The PAC

recognizes that (as was requested) compatibilities and synergies with GlueX were addressed in the resubmitted proposal and that the physics case was further refined. However, the physics of FCAL-II was considered too speculative to displace the GlueX program. Of course, the impact of a discovery in the proposed channels would be enormous; so as not to prevent these studies from running in the near future, we therefore ask that FCAL-II and the associated JEF physics program be fully incorporated to run in parallel with GlueX. We have thus given the experiment a C2 rating: approval of the physics case with the condition that JEF return to a later PAC with a convincing demonstration of their capabilities for running concurrently with GlueX.”

Based on these recommendations, we have been collecting $\eta \rightarrow 3\pi$ data in parallel with the GlueX experiment since 2015. A η/η' physics group was formed within the collaboration to analyze available GlueX data for the non-rare η decay channels. In the meantime, we also used the existing data to study the experimental backgrounds for the neutral rare decay measurements, such as $\eta \rightarrow 3\pi^0$ and non-resonant $2\pi^0$ production. A Monte Carlo simulation to test the experimental sensitivity of our key rare decay channel, $\eta \rightarrow \pi^0\gamma\gamma$, has been carried out under the GlueX high luminosity running conditions. These studies clearly demonstrate our capabilities to address the PAC42 recommendation “that FCAL-II and the associated JEF physics program be fully incorporated to run in parallel with GlueX”. In the following, we will summarize recent developments in the dark gauge boson search (our key search channel) and present our results from data analysis and Monte Carlo simulation for the experimental background and sensitivities. Motivations for the other decay channels and details of experimental design are described in the original proposal submitted to PAC42 [1].

III. MOTIVATION FOR SUB-GEV DARK GAUGE BOSON

About 80% of matter in the Universe is Dark Matter (DM)—whose constituents and interactions are unknown other than its gravitational properties. The simplest possible model for dark matter is a new stable Weakly Interacting Massive elementary Particle (WIMP). This has motivated a broad experimental program to detect non-gravitational DM interactions,

including direct searches for DM-nucleus scattering, indirect searches for DM annihilation products, and accelerator-based searches for missing energy. Due to the absence of evidence for WIMPs at the LHC and direct detection experiments, there is a strong consensus among the physics community [4] about the vital importance of broadening the scope of searches, both in the dark sector parameter space and in experimental approaches. Particularly, fixed-target experiments at high intensity frontiers offer a complementary approach to DM detection, with superior sensitivity to the sub-GeV dark sector. Recently the dark sector community report [4] recommended:

A broad experimental program, encompassing both DM direct detection experiments and accelerator-based searches for mediator force carriers as well as the DM particles themselves, has a tremendous potential to discover the new physics of the Dark Sector, revolutionizing our understanding of both particle physics and cosmology. We advocate that such a program be pursued with vigor and determination.

The stability of DM suggests that there may be a dark sector consisting of a rich symmetry structure with new forces and new particles. Dark sectors may include one or more mediator particles coupled to the SM via a portal. The portal relevant for dark sector-SM interactions depends on the mediator spin and parity: it can be a vector, a pseudoscalar, a fermion, or a scalar. The gauge and Lorentz symmetries of the SM greatly restrict the ways in which the mediator can couple to the SM. There are three dimension-4 portals: the vector, Higgs and neutrino portals from the SM sector into the dark sector (the additional axion portal is dimension-5 and suppressed by a high mass scale factor). The vector portal with additional $U(1)'$ gauge symmetry and an associated vector gauge boson is one of the best motivated extensions of the Standard Model [20]. A conserved charge can explain the stability of dark matter [21]–[25]. Since the corresponding current conserves all approximate SM symmetries, the coupling strength of DM to SM may exceed the SM weak scale without immediately running into strong constraints imposed by flavor physics and tests of discrete symmetries [26].

One model in the “Vector” portal from the SM sector into the dark sector that has been widely considered is a new force mediated by an abelian $U(1)'$ gauge boson A' (dark photon)

that couples very weakly to electrically charged particles through “kinetic mixing” with the photon [27]. Searching for a sub-GeV A' has drawn world-wide attention in recent years and has inspired a broad experimental program in the high-intensity frontier centers [4, 28]. Most of experimental searches for the A' rely on the leptonic coupling of this new force (for example, detecting its decays to e^+e^- or $\mu^+\mu^-$). There are four experiments of this type at Jefferson Lab: APEX [29], HPS [30], DarkLight [31], and the recently developed BDX [32].

Another equally compelling model in the “Vector” portal not covered by the dark photon searches is a new force mediated by a leptophobic gauge B' -boson that couples predominantly to quarks and arises from a new $U(1)_B$ baryon number gauge symmetry [33, 34]. The $U(1)_B$ local gauge symmetry was initially proposed by Lee and Yang back in 1955 [35] and subsequently discussed extensively in the literature [25, 33, 34, 36, 37]. A new $U(1)_B$ gauge symmetry provides a natural frame-work for the Peccei-Quinn mechanism in the quark sector for solving a long standing “strong CP problem” [36]. This model has also been motivated in part by the similar cosmological abundances of dark matter and baryonic matter in the Universe, which may point toward a unified baryogenesis mechanism for both types of matter [40]. New baryonic fermions with electroweak quantum numbers are required to cancel the $SU(2)_L^2 \times U(1)_B$ and $U(1)_Y^2 \times U(1)_B$ anomalies. The new fermions acquire masses (Λ) via a $U(1)_B$ -breaking Higgs field, with $m_B/\Lambda \geq g_B/(4\pi)$ [41], where m_B is the mass of B' -boson and g_B is the $U(1)_B$ gauge coupling.

A new physics motivation for sub-GeV mass mediator force carriers comes from the host of observational questions related to the dark matter sub-structure. Even though the paradigm of Cold Collisionless DM (CCDM) has been extraordinarily successful in explaining astrophysical observations of structure, such a model does not agree with several observations of the characteristics of dwarf galaxies [9]. Issues concerning the small-scale structure of the universe can be alleviated if the DM particles occupying the halos can elastically scatter with other DM particles. In order for the self-interaction cross section to be large enough to explain these observations, the mass of the mediator particle must be small relative to the weak scale; a typical range is $\sim\text{MeV–GeV}$ [8, 9]. It is demonstrated in [8] that self-scattering of $\sim\text{GeV–TeV}$ DM particles via a sub-GeV mediator can simultaneously explain the DM relic abundance during freeze-out and solve small scale structure anomalies in dwarf galaxies and subhalos, while satisfying constraints on larger galaxy and cluster scales.

The search for a sub-GeV leptophobic B' -boson is a top priority physics goal for this proposal. It will be complementary to the searches based on the dark photon or the other leptophilic models.

IV. RECENT EXPERIMENTAL DEVELOPMENTS FOR LEPTOPHOBIC B' SEARCH

The experimental signatures for B' and dark matter depend on its mass m_B and decay channels. If the dark matter particle mass follows $m_\chi < m_B/2$, the best experimental probe is through invisible decays of mesons or in hadron beam dump experiments. Recently there are several new initiatives in the field. Pospelov et al. suggested to search for a sub-GeV B' and dark matter at neutrino factories such as MiniBooNE with a projected sensitivity to baryonic fine structure constant down to $\alpha_B \sim 10^{-6}$ [26]. Dobrescu and Frugiuele [46] proposed to search for B' in the mass range of 1–10 GeV by using a ~ 100 GeV proton beam from the main injector at Fermilab scattering off a fixed target to produce a dark matter beam, then detecting it with the NO μ A near detector. A very recent proposal aims to explore a possible B' at a few TeV mass range in the semi-visible jets at LHC [39].

If the dark matter particle mass follows $m_\chi > m_B/2$, a direct search for B' directly through observation of the visible final states [26] provides more sensitivity and this is a main focus of the JEF experiment described below. Experimental searches for leptophobic bosons at hadron colliders over the last few decades have set upper limits on their couplings for masses in the 50 GeV to 3 TeV range [7, 38, 42]. Masses smaller than the pion mass also have very strong constraints from searches for long-range nuclear forces [43]. However, masses around the QCD scale have been nearly “untouched” due to large SM backgrounds [38]. Nelson and Tetradis first proposed to search for a sub-GeV B' -boson through η decays in 1989 [33]. They assumed that $B' \rightarrow \pi^+\pi^-$ would dominate for $m_B > 2m_\pi$. In that case, the signal of sub-GeV B' would be mostly hidden under the ρ meson decay. Tulin demonstrated in his recent article [34] that $B' \rightarrow \pi^+\pi^-$ is suppressed due to G-parity conservation and the leading decay channel is $B' \rightarrow \pi^0\gamma$ for $m_\pi \leq m_B \leq 620$ MeV and $B' \rightarrow \pi^0\pi^+\pi^-$ for $m_B > 620$ MeV. This offers a unique experimental opportunity to search for B' in the mass

range $m_\pi < m_B < m_\eta$ through the doubly-radiative decay $\eta \rightarrow \pi^0\gamma\gamma$. The new physics decay $\eta \rightarrow B'\gamma \rightarrow \pi^0\gamma\gamma$ would produce a resonance peak at m_B in the $\pi^0\gamma$ invariant mass distribution, while the SM-allowed $\eta \rightarrow \pi^0\gamma\gamma$ decay with a suppressed branching ratio of $\sim 2.7 \times 10^{-4}$ [7] would be present as an irreducible background in the signal window.

There is a very recent result published by the Belle collaboration [47] describing a search for the B' -boson via the $\eta \rightarrow B'\gamma \rightarrow \pi^+\pi^-\gamma$ channel, since the leading decay mode of $\pi^0\gamma$ suffered from high combinatoric background in their data and was not used in the analysis. Only a moderate constraint of 10^{-3} – 10^{-2} on the baryonic fine structure constant was obtained for the B' mass range of 0.29–0.52 GeV.

The JEF experiment will search for the B' -boson in the mass range of 0.14–0.54 GeV through $\eta \rightarrow \gamma + B' \rightarrow \gamma + \gamma\pi^0$. The experimental sensitivity with 100 days of beam time is shown in Fig. 1. This figure was taken from our original proposal [1]; our studies for the running conditions described below in this update suggest that we should be able to attain a similar reach. This measurement will improve the existing bounds by two orders of magnitude, with sensitivity to the baryonic fine structure constant α_B as low as 10^{-7} , indirectly constraining the existence of anomaly-canceling fermions at the TeV-scale. The JEF search for a B' -boson is complementary to other accelerator-based searches for invisible B' decays, such as the newly proposed program at the MiniBooNE neutrino factory [26]; it is also complementary to ongoing worldwide search for a dark photon focusing mainly on signatures involving lepton coupling.

V. UNIQUE FEATURES OF JEF EXPERIMENT IN η DECAYS

In recent decades, using η decays as tests for SM physics and as probes for BSM new physics has drawn attention from the physics community world-wide. There have been intensive experimental activities across different facilities using different production mechanisms and experimental techniques with complementary energies.

BEPC-II in China and DAΦNE in Italy are e^+e^- collider facilities operating with symmetric and relatively low energy e^+ and e^- beams with designed luminosity of $\sim 10^{33}$ cm⁻²s⁻¹. The

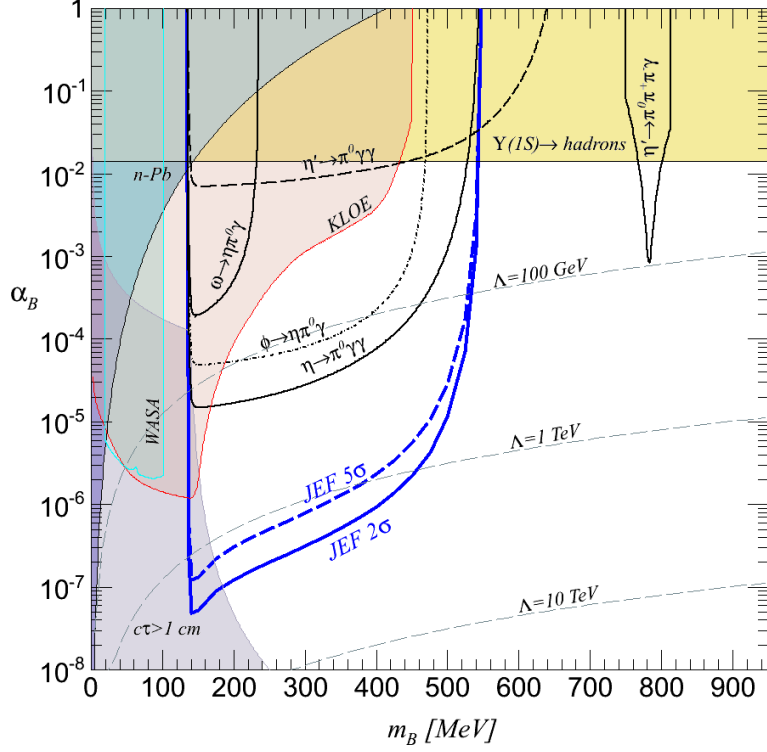


FIG. 1: Current exclusion regions for a leptophobic gauge B' -boson [34], with the projected JEF search region for the baryonic fine structure constant versus mass plane. Shaded regions are exclusion limits from hadronic $\Upsilon(1S)$ decay [42] and low energy n - Pb scattering [43]. The pink and blue shaded regions are from the dark photon A' searches (KLOE [44] and WASA [45]). The A' limits applied to B' are model-dependent, constraining possible B' leptonic couplings. Limits shown here are for the leptonic couplings of $\epsilon = 0.1 \times eg_B / (4\pi)^2$. The black contours are current exclusion limits from radiative light meson decays based on their total rate (assuming the QCD contribution is zero). The light purple shaded region shows where B' has a macroscopic decay length $c\tau > 1$ cm. The solid blue curve shows the projected 2σ sensitivity and the dashed blue curve shows the projected 5σ sensitivity for the JEF experimental reach. Dashed gray contours denote the upper bound on the mass scale Λ for new electroweak fermions needed for anomaly cancellation.

BESIII collaboration at BEPC-II [48] and the KLOE-II collaboration at DAΦNE [49] have recently collected large η data samples through vector meson radiative decays ($J/\psi(3097)$ for BESIII and $\phi(1020)$ for KLOE-II, respectively). KLOE-II has become one of the leading η meson factories [50], while BESIII offers access to both η and η' production due to a

larger center-of-mass (c.m.) energy. Another e^+e^- collider, VEPP-2000 [51], with a smaller designed luminosity of $\sim 10^{32} \text{ cm}^{-2}\text{s}^{-1}$ and a c.m. energy up to 2 GeV has been operating since 2010. A magnetic detector (CMD-3 [52]) and a nonmagnetic detector (SND [53]) installed in two interaction regions of VEPP-2000, have already collected an integrated luminosity of $\sim 60 \text{ pb}^{-1}$. A goal of $\sim 1 \text{ fb}^{-1}$ is expected in the coming decade. Two B factory experiments, the Belle experiment [54] at the KEKB collider in KEK and the BaBar experiment [55] at the PEP-II collider in SLAC, had produced η 's through the two-photon fusion reaction. Both colliders have asymmetric positron and electron beam energies (4.0 GeV and 7.0 GeV for KEKB, 3.1 GeV and 9 GeV for PEP-II, respectively) to boost the produced particles in the lab frame, offering opportunities to study the dynamic properties of $\eta^{(\prime)}$ at Q^2 up to 100 GeV^2 . After a decade of running, PEP-II was turned off in 2008. The KEKB collider and the Belle detector, on the other hand, are being upgraded to SuperKEKB and Belle-II. More statistics will be expected from Belle-II in the coming decade [56].

There are also several on-going fixed-target experimental programs. The A2 collaboration at MAMI has been playing one of the leading roles in studying $\eta^{(\prime)}$ decays involving electromagnetic particles in the final state. A high precision tagged photon beam was used to produce $\eta^{(\prime)}$ near the threshold through the $\gamma p \rightarrow \eta^{(\prime)} p$ reaction. The electromagnetic particles from $\eta^{(\prime)}$ decays were detected by a nonmagnetic detector that combines two electromagnetic calorimeters, a spherical Crystal Ball covering $\sim 93\%$ of 4π and a forward TAPS detector covering the small polar angles from 1° to 20° [57]. The WASA-at-COSY collaboration used the hadronic production of $\eta^{(\prime)}$ on an internal pellet target (frozen hydrogen or deuterium) at the cooler synchrotron COSY storage ring [58], Germany. A large η -data sample has been produced in the proton-nucleus fusion reaction $pd \rightarrow \eta {}^3\text{He}$ ($\sim 3 \times 10^7 \eta$ [60]) or $pp \rightarrow \eta pp$ ($\sim 10^9 \eta$ [61]) with a proton beam energy slightly above the threshold; the η 's were tagged by measuring the recoil nucleus in the forward WASA detector (3° – 18°) [59]; and the decay particles of $\eta^{(\prime)}$ were detected by a central detector system (20° – 169°) with a superconducting solenoid magnet. In addition, there have been also active investigations of $\eta^{(\prime)}$ in high energy fixed target experiments, such as the NA60 experiment [62] using a 400 GeV proton beam at the Super-Proton-Synchrotron (SPS) in the CERN North Area, and the LHCb experiment [63] at Large Hadron Collider (LHC). Most recently, there has been a ‘‘Rare Eta Decays with a TPC for Optical Photons’’ experiment (REDTOP) under development

at Fermi Lab [64]. The physics goal of REDTOP experiment will have some overlap with the JEF experiment but with more emphasis in the charged decay channels (while JEF will have more emphasis on the neutral channels with a factor of two better energy resolution for photons). The η 's will be produced by a ~ 1.8 GeV proton beam on Nb and Be nuclear targets. Due to the nature of hadronic production, a high production rate is expected at level of 2×10^{12} η 's per year; the background level will be high as well. According to [64], a proposal will be submitted to Fermi Lab PAC in 2018. If it is approved, a new beam line and new experimental hall will be constructed.

Compared to the other η experiments described above, the unique features of the JEF experiment at JLab are: (1) highly boosted η 's are produced by a ~ 12 GeV tagged photon beam through the $\gamma p \rightarrow \eta p$ reaction; (2) η 's are tagged by measuring the recoil proton; and (3) the electromagnetic particles from the η decays (γ , or e^+ and e^- in some cases) will be measured by a state-of-the-art, high resolution, hybrid FCAL-II calorimeter with a central insertion of high granularity PWO crystals (shower overlaps will be significantly suppressed). The decayed products from a highly boosted η have relatively high energies therefore their detection will be significantly less sensitive to the detector threshold effects compared to those experiments where the η 's have relatively low kinetic energies in the lab frame. The η decay particles in the JEF experiment will be mostly concentrated in the forward direction and be detected by FCAL-II. Using the existing Barrel CALorimeter (BCAL) as a veto detector will help to effectively reject background channels for (for example) the $\eta \rightarrow \pi^0 \gamma \gamma$ channel with more than four final state photons (such as $\eta \rightarrow 3\pi^0$) migrating into the signal channel with less final state photons, which will be demonstrated in the next section. The combination of all these experimental techniques in the JEF experiment will offer unprecedented low backgrounds for η rare decays, particularly for neutral decay modes, with up to a factor of two orders of magnitude reduction in backgrounds compared to all other existing or planned experiments in the world. The result from the JEF experiment will provide the most stringent constraint for B' in the mass range of 140–550 MeV through the $\eta \rightarrow \gamma B' \rightarrow \gamma \gamma \pi^0$ reaction, as shown in Fig. 1. On the other hand, the GlueX apparatus, a solenoid magnet with tracking detectors and time-of-flight walls, offers excellent capability to detect charged particles, such as pions and electrons, as well. One can also search for new physics in complementary processes, such as searching for B' with a mass $m_B < m_\pi$

through $\eta \rightarrow \gamma B' \rightarrow \gamma e^+ e^-$ since $B' \rightarrow e^+ e^-$ will dominate in this mass region [34]. In the event of a discovery for $m_B < m_\pi$, one can distinguish the B' from the dark photon A' by studying ω decays: $\omega \rightarrow \pi^0 A'$ can occur while $\omega \rightarrow \pi^0 B'$ is highly suppressed by isospin conservation, according to Tulin [65]. A light pseudoscalar or scalar meson can also be probed through $\eta \rightarrow \pi^0 H \rightarrow \pi^0 e^+ e^-$ [66]. In addition, the same experimental data will also offer an opportunity to search for B' in the direct photo-production $\gamma p \rightarrow B' p$ process, as pointed out by C. Fanelli and M. Williams [67]. The projected sensitivity for the direct production of B' during the GlueX Phase IV run period is shown as a red dotted curve in Fig. 2, which covers a broad B' mass range up to 1 GeV.

The projected η production rate for JEF is at the level of $\sim 6 \times 10^7$ per 100 days (assuming photon beam energy $E_\gamma > 8$ GeV). It will not be the highest η production rate compared to some other experiments, such as the REDTOP experiment. However, it will certainly be leading in the clean background frontier, particularly in the η neutral decay mode. The JEF experiment can be run in parallel to the other experiments in Hall D, such as the GlueX and PrimEx-eta experiments, or any future experiments using a hydrogen target. This offers the possibility to continuously accumulate data throughout the JLab 12 GeV era. In addition, the production rate for η' is about the same as η for the beam energy range planned for the JEF program. The same data set will allow studies of both η and η' decays in the same setting. The results from these comprehensive studies of η - η' sector will have a great potential to make a significant impact in our understanding of low energy QCD and new physics beyond SM.

VI. EXTENSION TO η' PHYSICS

Multiple ongoing GlueX analyses have confirmed that photo-production rates for the η and η' are similar, suggesting that GlueX could become a competitive facility for η' studies. Rare but allowed, photon-rich decays of the η' which have not yet been observed are $\pi^0 2\gamma$ ($BR < 8 \times 10^{-4}$), $\eta 2\gamma$ (BR not listed), and $4\pi^0$ ($BR < 3.2 \times 10^{-4}$) [68]. Although the acceptance in FCAL-II for photons from η' decays will be smaller than for the lighter η , the construction of FCAL-II will likely improve measurements of rare, photon-rich decays of

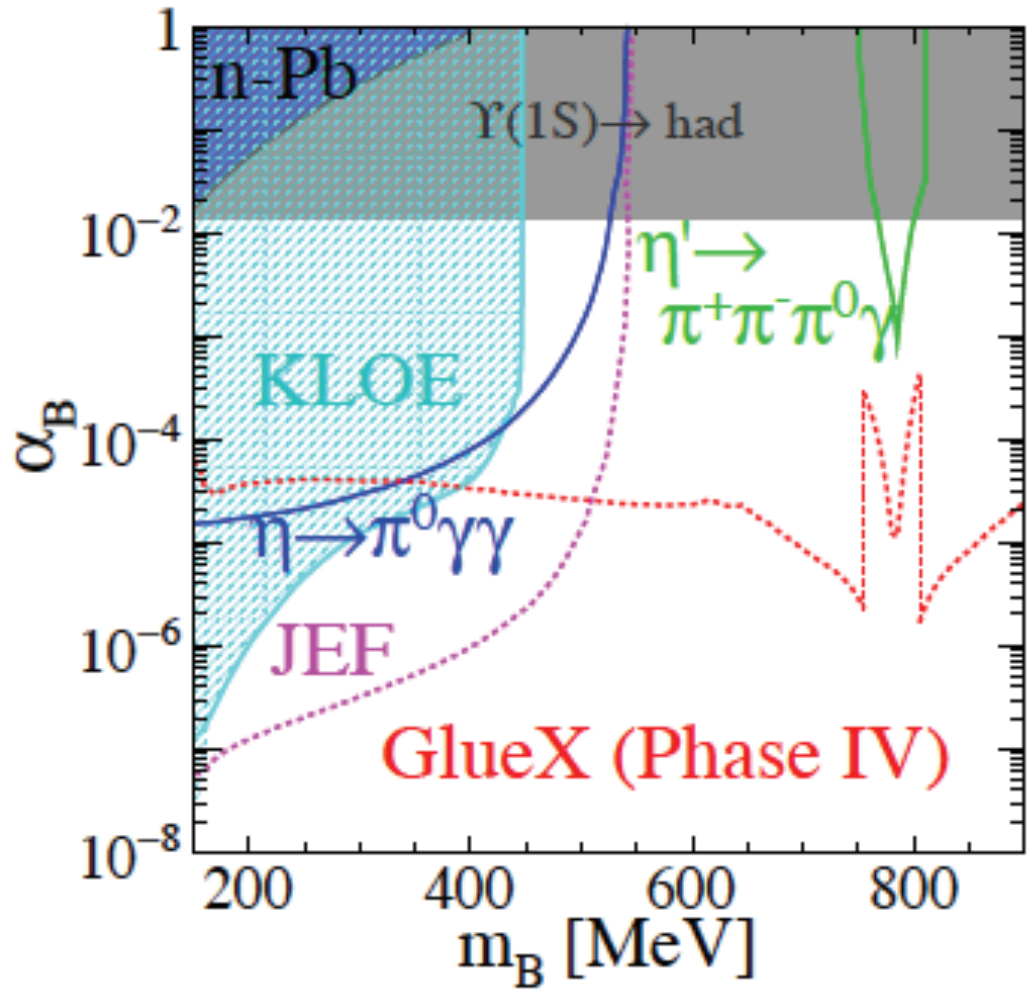


FIG. 2: Current exclusion regions for a leptophobic gauge B' -boson [34], compared to the expected sensitivity from the η decay at JEF and the direct photoproduction (red dotted curve). The figure is taken from [67].

the η' by reducing backgrounds from missing photons as well as combinatoric backgrounds. We have not done simulations for η' decays with FCAL-II, but discuss in the following paragraphs what measurements might be pursued.

An η' physics program could search for the four-photon decay channels, $\pi^0 2\gamma$ and $\eta 2\gamma$. As in the case of $\eta \rightarrow \pi^0 2\gamma$, scalars are expected to make significant contributions in these decays [69]. It is encouraging that the calculated branching ratios are near current experimental limits. A background that will be important due to missing photons is $\eta' \rightarrow \eta 2\pi^0$ (BR=22.3%) $\rightarrow 6\gamma$. The $\eta' \rightarrow 4\pi^0$ decay leading to 8 photons is not expected to be accessible in GlueX since one calculation estimates the branching ratio to be 4×10^{-8} [70]. Here the goal would be to lower the BR upper limit below the current 3.2×10^{-4} to test the prediction that this decay is indeed heavily D-wave suppressed (i.e., that there are no unexpectedly large contributions from a pair of tensor mesons, for example). It should be possible to avoid the large potential background from $a_0(980) \rightarrow \pi^0 \eta$ by excluding events with combos in which $M(3\pi^0) \sim M(\eta)$. Finally, a photon-rich decay of the η' that is effectively SM forbidden is $\eta' \rightarrow 3\gamma$ ($BR < 1.0 \times 10^{-4}$) [68], a test of C invariance. Again, FCAL-II would reduce what are almost certainly important backgrounds from $\eta' \rightarrow \eta 2\pi^0$ (BR=22.3%) with missing photons.

VII. HYBRID CALORIMETER FCAL-II

The JEF program will use the existing beam line and detector array of the current GlueX experiment with a modification to the forward calorimeter (FCAL). The plan is to replace the inner part of the existing FCAL (composed of $4 \times 4 \times 45 \text{ cm}^3$ lead glass blocks) with lead tungstate crystals with a smaller $2.05 \times 2.05 \times 18 \text{ cm}^2$ size. In section III.A of the original proposal (PR12-14-004) [1], we demonstrated that an upgraded FCAL-II is essential for rare neutral η decay measurements. The size of $1.2 \times 1.2 \text{ m}^2$ for a PWO crystal insertion was proposed in PR12-14-004 [1].

For our key signal channel $\eta \rightarrow \pi^0 \gamma \gamma$, a potentially dangerous background comes from $\eta \rightarrow 3\pi^0$ since it may form a peak under the signal window in the 4γ invariant mass distribution if there are two overlap showers in the calorimeter from different pairs of decay photons. All

other sources of background will have flat distributions in the signal window. Therefore, we use this background channel to optimize the size for the insertion while maintaining a similar experimental sensitivity as projected in the original proposal. We define a figure-of-merit given by

$$FOM = \frac{N(\eta \rightarrow \pi^0 \gamma \gamma)}{\sqrt{N_b(\eta \rightarrow 3\pi^0)}}. \quad (1)$$

The figure-of-merit as function of the size of the insert is shown in Fig. 3. We found that we can obtain the same figure-of-merit we obtained for the original $1.2 \times 1.2 \text{ m}^2$ profile presented in PR12-14-004 [1] for an insert with a $1 \times 1 \text{ m}^2$ profile if we veto events with showers in the BCAL with energies more than 30 MeV.

A. Update on FCAL-II, cost, and manpower

As discussed above, using BCAL as a veto detector will effectively help us to improve the signal-to-noise ratio. In order to optimize the cost and the experimental Figure-Of-Merit (FOM), we modified the size of the PWO crystal insertion from $1.2 \times 1.2 \text{ m}^2$ described in the original proposal [1] to a smaller size $1 \times 1 \text{ m}^2$ in this updated version. Therefore, the number of the crystal modules required for FCAL-II will be 2464 instead of 3445 as stated in the original proposal, which will save about 30% in cost and manpower for the detector development. On the other hand, the cost of PWO crystal has increased significantly over the past several years (\$790 per crystal module compared to \$250 quoted in the original proposal [1]). An update on the crystal insertion cost is summarized in Table II. We expect that the infrastructure costs (such as support structure, cables and panels) will be provided by JLab so that these items are not included in this estimate.

As pointed out in our original proposal [1], FCAL-II is similar to a larger version of the state-of-the-art, high-resolution PrimEx calorimeter (HyCal) used in Hall B. Several institutions on this proposal were major players in the design and construction of HyCal and would play a leading role in developing the future FCAL-II. Previously, we successfully obtained the resources necessary to develop and construct HyCal from the NSF Major Research Instrumentation (MRI) program while establishing collaborations with Chinese institutions. The same strategy would be applied to the FCAL-II development.

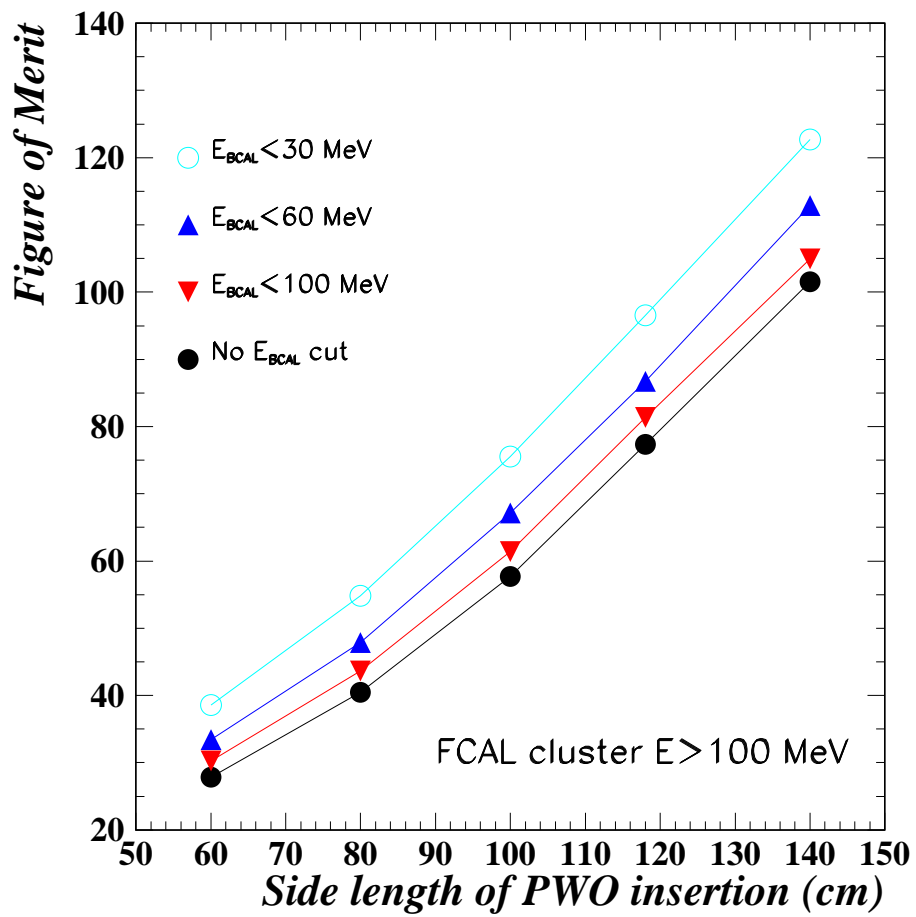


FIG. 3: Figure-of-merit for optimization of insert size.

Item	Channels	Unit Cost	Cost
PWO crystal	2464	\$790	\$1.95M
PMT+base+house	2464	\$450	\$1.11M
Flash ADC	2464-616=1848	\$378	\$0.70M
HV	2464	\$300	\$0.74M
Total			\$4.50M

TABLE II: The estimated cost for FCAL-II. Note: About 616 lead glass modules in the existing FCAL will be replaced by the PWO counters. The flash ADCs for these lead glass detectors will be recycled for use with the PWO counters.

The estimated total cost for 2464 PWO crystal modules, including the crystal, PMT/base, flash ADC and HV, is about \$4.5M. Our Chinese collaborators, leading by prof. X. Chen, will apply for funds (\sim \$1.0M) from the Chinese National Science Foundation to cover the cost of the crystals. Prof. L. Gan (spokesperson of this proposal) will lead the US institutes in applying for a Major Research Instrumentation program (MRI) grant from the National Science Foundation (\$1.0M-\$3.5M) to cover the cost of PMT's, bases, possibly the Flash ADCs, plus small ancillary detectors. The other co-spokespersons are JLab staff members and will help coordinate design and construction. We would like the power supplies, cabling, possibly the Flash ADCs, and other readout support to come from JLab. We will need design and engineering support for infrastructure (*e.g.* frame, support structure, cooling system, etc.), as well as support from the Physics Division electronics group in designing low power PMT bases.

This experiment has the potential to add new manpower to the Hall-D effort, in particular from groups that historically had little activity at Jefferson Lab. During the detector development and construction period, the Chinese team will be responsible for procuring and testing the PWO crystals. The US team will be responsible for the procuring and testing of the electronics. Several local universities near Jlab will play a major role in the detector assembly and testing.

B. Impact of FCAL-II Installation on the Run Schedule in Hall D

Assuming this proposal is approved, we need at least one year to obtain external funding for the calorimeter upgrade. According to our communication with the Shanghai Ceramics Institute, manufacturing of 2464 PWO crystals requires about 2–3 years. We estimate an additional one year to assemble all the crystal counters. In the best scenario, about five years are required in order for the crystal counters to be assembled and ready for installation. Therefore, the earliest date for FCAL-II installation is projected to be in 2023. On the other hand, the total number of beam days approved for the GlueX program is 540 days: 120 days for E12-06-102, 200 days for E12-13-003, and 220 days for E12-12-002. Some initial runs for E12-06-102 were carried out in 2016 and 2017. Both E12-13-003 and E12-12-002 are proposed to study meson and baryon decays to strange final states and are expected to overlap in time. Therefore, we estimate that there are actually ~ 300 beam days remaining for GlueX to run in the coming years. In addition, there are two other approved experiments in Hall D. One is a Primakoff experiment to measure the η radiative decay width (E12-10-011) with 79 beam days and the second is the charged pion polarizability measurement (E12-13-008) with 25 beam days. The total number of remaining beam time for all approved experiments in Hall D is roughly ~ 400 days, which is very likely to be completed by the end of 2022. In the event of new discoveries during the GlueX run, it will be highly desirable to have a high resolution calorimeter to extend the GlueX program for high precision measurements. Furthermore, after several years operating in a high intensity photon beam environment, the lead glass modules in the central part of FCAL will also require refurbishment due to radiation damage. Therefore, the year of 2023 will be a good time window for an upgrade to FCAL that will have minimal impact on the run schedule in Hall D. The estimated time for the FCAL-II installation is about one year depending on how many bad lead glass modules from the current FCAL need to be refurbished. The detailed estimated schedule for FCAL-II installation is summarized in Table III. We estimate that about four-person manpower will be required during the installation.

Activities	time (month)
Disconnect cables, disassemble FCAL and inspect lead glass counters	2
Install additional 2000 channels of cable and electronics	1
Stack FCAL-II counters, refurbish some bad lead glass counters	6
Connect cables, monitoring system, cooling system	1
Final check-out	2
Total	12

TABLE III: The estimated schedule for FCAL-II installation in Hall D.

VIII. SIMULATION OF THE $\eta \rightarrow \pi^0 \gamma \gamma$ SIGNAL

The geometry for a $1 \times 1 \text{ m}^2$ insert within the FCAL was implemented into the simulation of the GlueX detector; a visual representation of a single 4γ event is shown in Fig. 4. Signal events for the reaction $\gamma p \rightarrow p\eta$ were produced using a generator based on a Reggeon-exchange model by Laget [71], which also includes Primakoff production. We used phase space for the decay of the η . We modeled the running conditions for GlueX Phase-IV (see Table VI in [2]). The incident beam photons were generated according to a coherent bremsstrahlung spectrum with the coherent peak at 9 GeV and an endpoint energy of 12 GeV; the spectrum is shown in Fig. 5. We assumed that the lower-photon-energy part of the tagger for high-intensity running would be turned off and applied a minimum beam energy of 6 GeV. The generated events were passed through a full Geant3-based Monte Carlo of the GlueX detector, including the material and geometry for the insert. The material for the DIRC was also included. The proton tracks mostly head into the CDC but must first pass through the target matter, the target scattering chamber (composed of low-density foam) and the start counter; this leads to an effective cut-off in the proton momentum at about 250 MeV/c. Protons are identified via a combination of energy loss in the chambers and time-of-flight to the Barrel Calorimeter. The acceptance for the proton is shown in Fig 6. The efficiency rises sharply from the threshold of about 250 MeV/c and exceeds 95% above about 350 MeV/c. The overall efficiency for proton detection is about 67%. Photons were reconstructed in the BCAL (with a shower threshold of 30 MeV) and the hybrid FCAL (with

FCAL view from downstream looking upstream

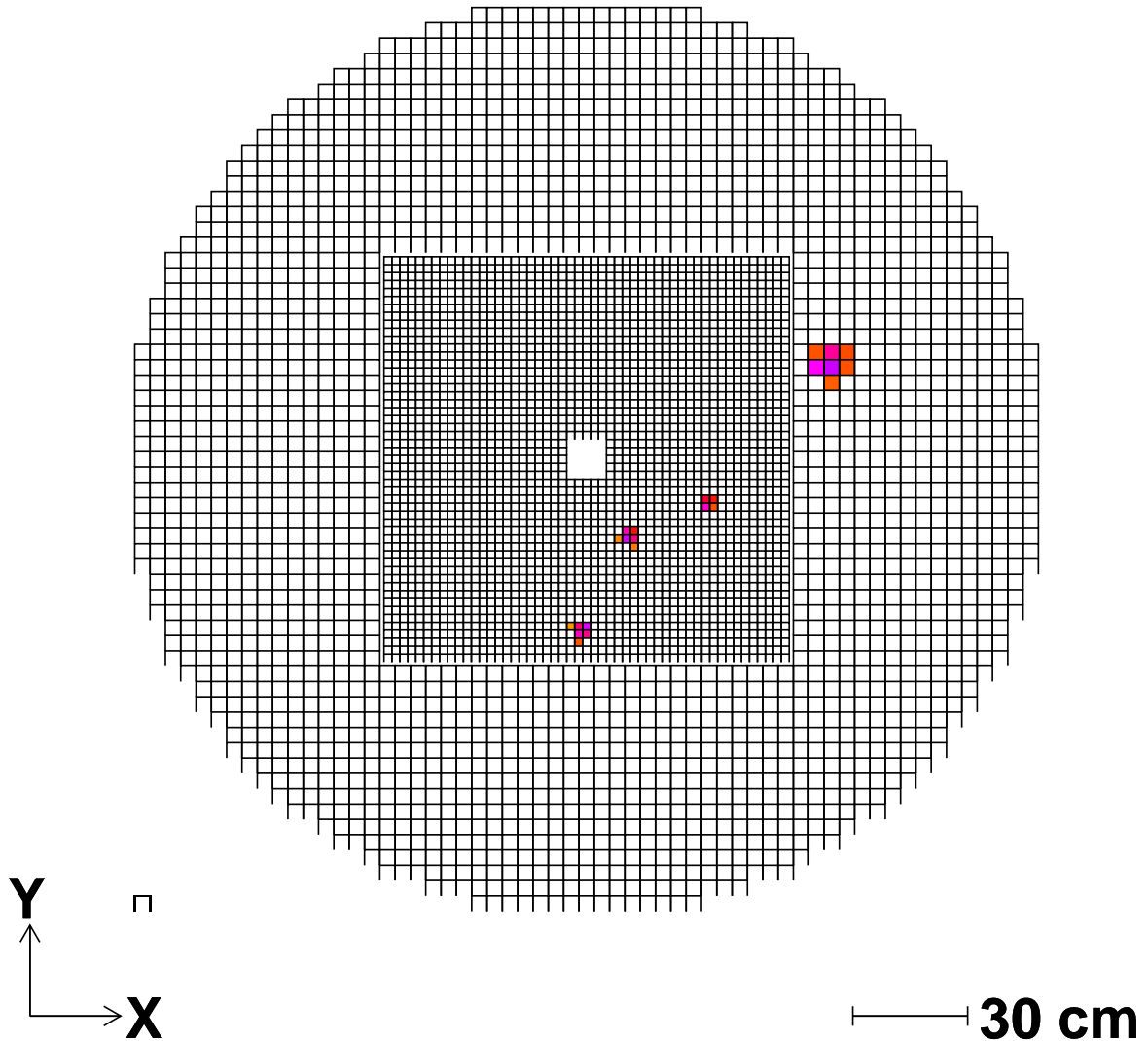


FIG. 4: Hybrid calorimeter in the simulation showing a sample $\eta \rightarrow \pi^0\gamma\gamma$ event.

a shower threshold of at least 100 MeV). The reconstructed energy balance and co-planarity between the proton and the four photons from the decay of the η are shown in Fig. 7. Events for which $|\Delta E| < 0.44$ GeV and for which $\Delta\phi$ is within $\pm 5^\circ$ of 180° are accepted for further analysis. Events with showers within the inner “ring” of blocks around the beam hole were excluded. Most of the photons end up in the FCAL, as shown in Fig. 8. The showers in the BCAL tend to correspond to lower-energy photons that have poor energy resolution; some photons head toward the gap between the FCAL and the BCAL where

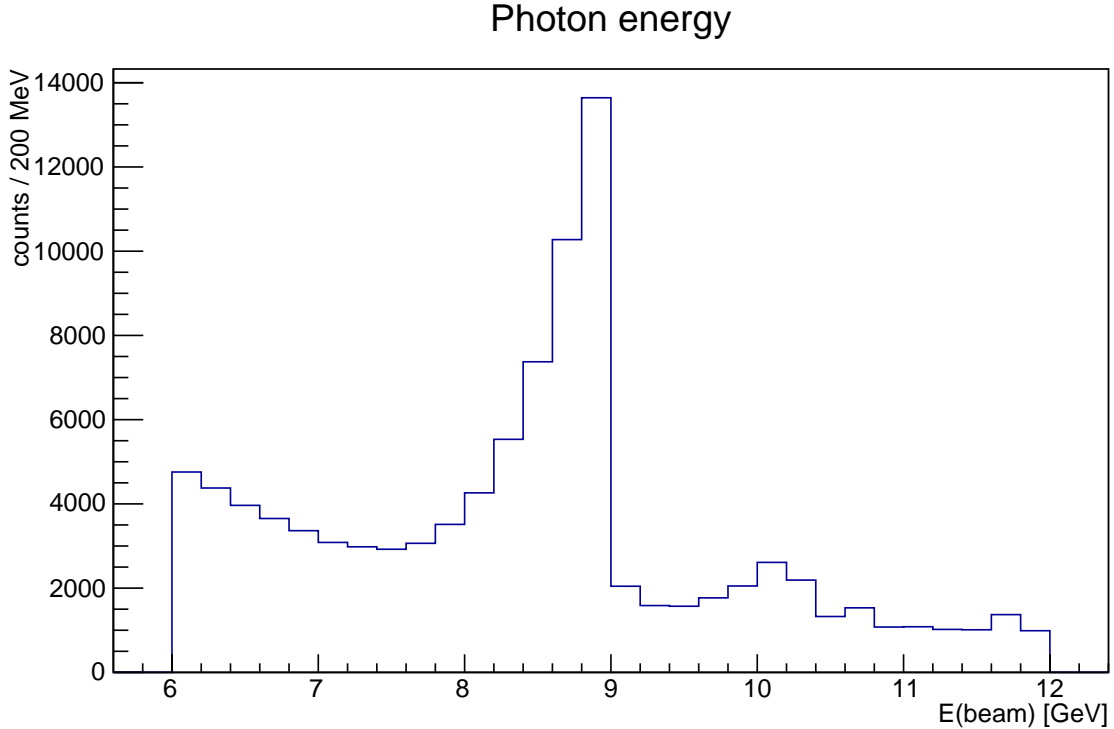


FIG. 5: Photon beam energy spectrum for 100,000 generated events.

some of the energy is lost. For these reasons we plan to veto events with showers in the BCAL. The effect on the mass resolution is shown in Fig. 9 and the effect on the efficiency is demonstrated in Table IV. For the case where all the photons are in the FCAL (including the insert) the mass resolution is about 13.7 MeV when the FCAL threshold is 0.1 GeV. The two-photon invariant mass distribution showing the quality of the π^0 reconstruction under these conditions is shown in Fig. 10. Raising the threshold to 0.5 GeV reduces the asymmetric shape of the π^0 peak; for this case, the resolution of the π^0 peak is about 4.6 MeV. The beam energy threshold in the analysis needs to be tuned; we are currently using a rough range of 8–12 GeV.

IX. BACKGROUND SIMULATIONS

A large source of background comes from $\eta \rightarrow 3\pi^0$ where two photons are either lost or nearby clusters are merged together. The leakage into the 4γ mass spectrum is small compared to the number of events where all six photons from (two from each π^0) are recon-

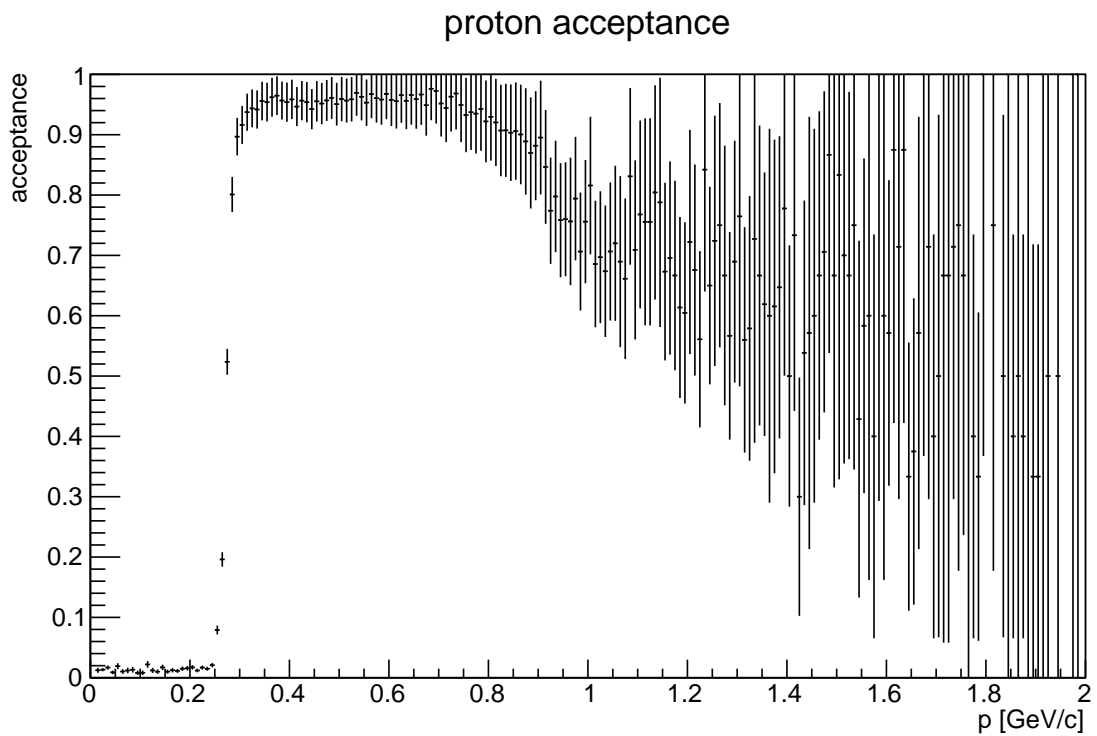
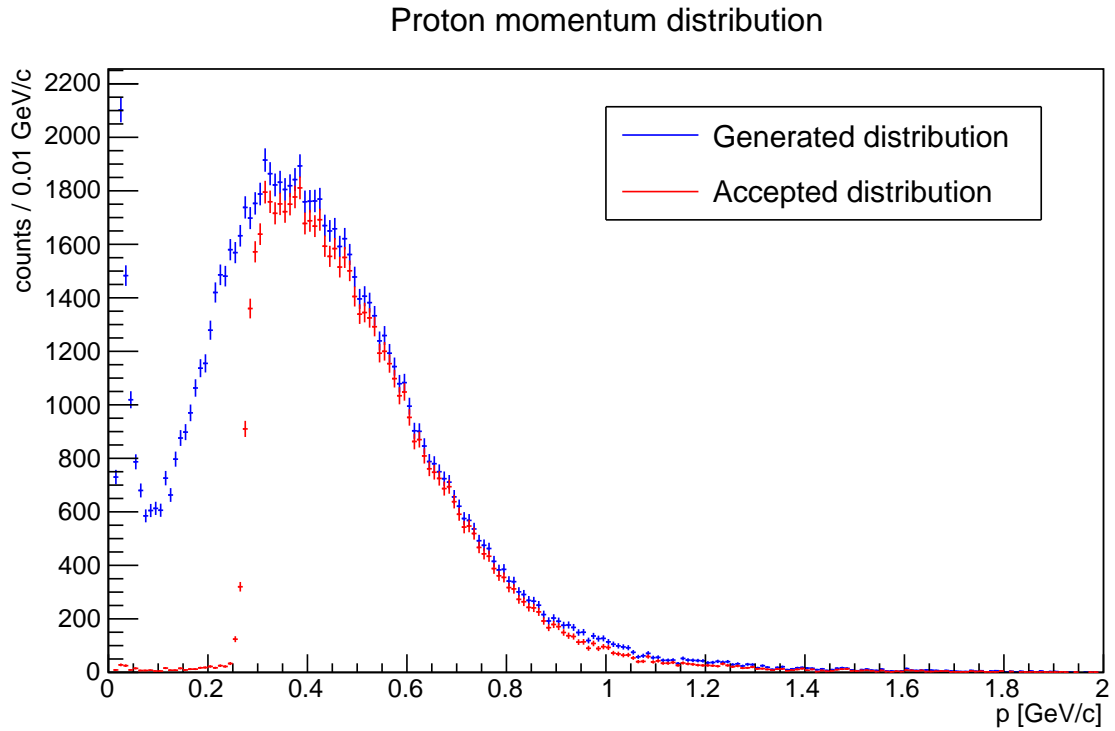


FIG. 6: The thrown and reconstructed/accepted proton momentum distribution is shown in the top panel. The peak at very low momentum is from the Primakoff events and the hump at 0.4 GeV/c arises from ρ and ω Reggeon exchanges. The proton acceptance is shown in the bottom panel.

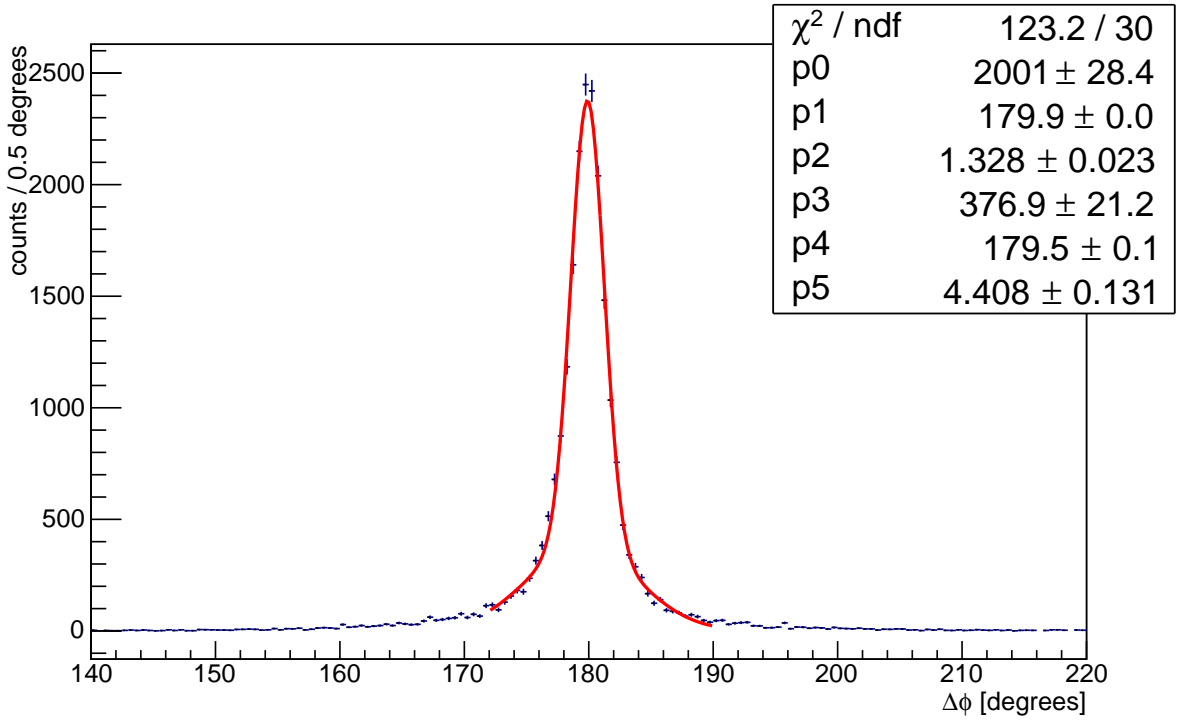
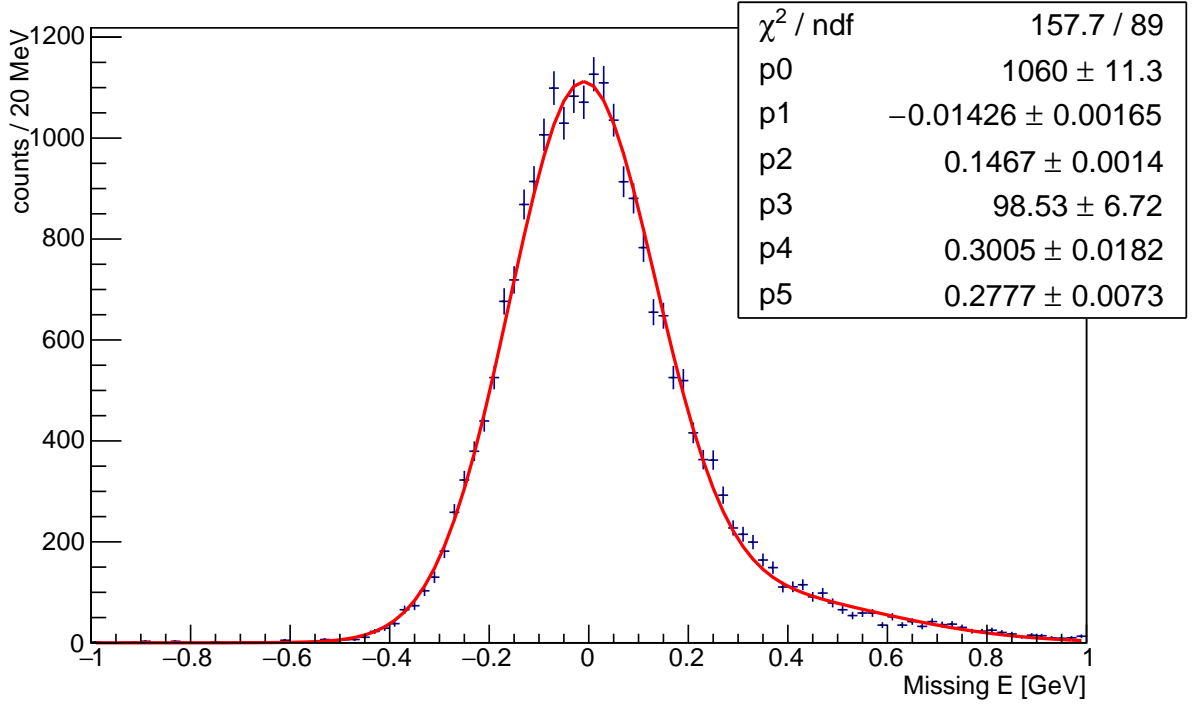


FIG. 7: The energy balance (missing energy) is plotted in the top panel and the co-planarity ($|\phi_{4\gamma} - \phi_p|$) is shown in the bottom panel for the reaction $\gamma p \rightarrow p\eta$, $\eta \rightarrow \pi^0\gamma\gamma$. The threshold in the FCAL was 0.1 GeV.

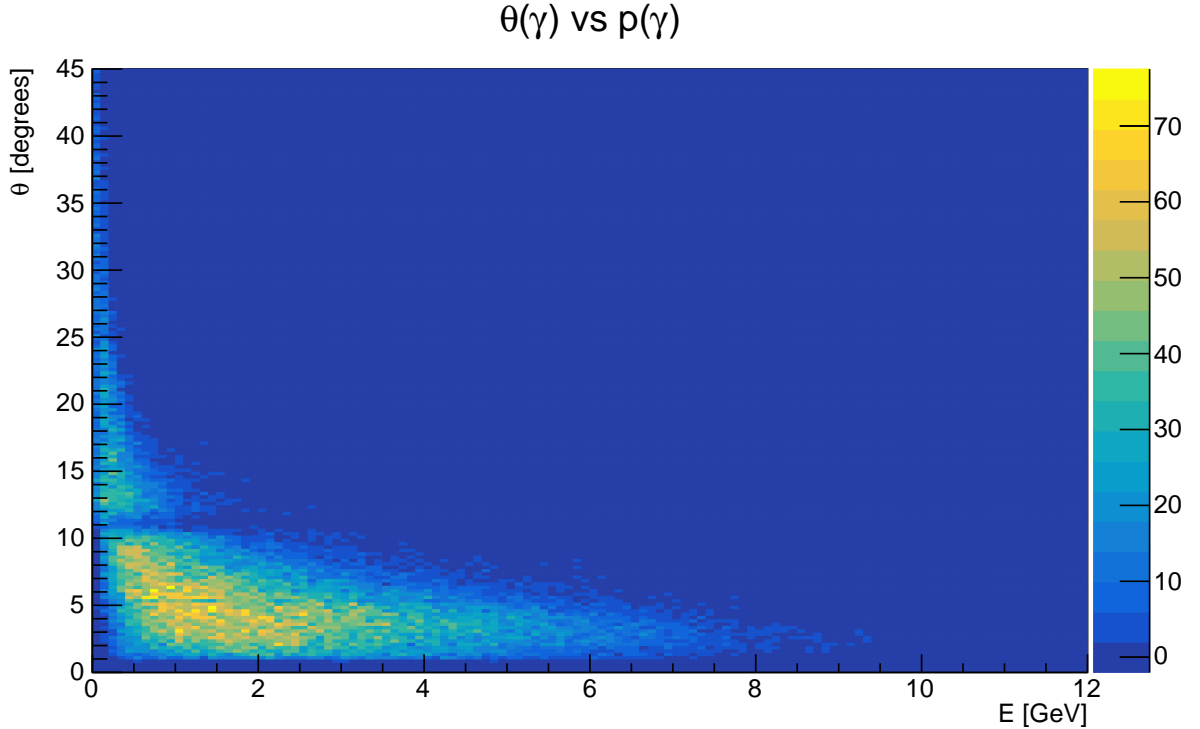


FIG. 8: Relationship between energy and angles of photons from $\eta \rightarrow \pi^0\gamma\gamma$. The dip in counts at about 11° corresponds to the gap between the end of the BCAL and the FCAL. The threshold in the FCAL was 0.1 GeV.

structured (see Fig. 11), but the ratio of the branches $BR(3\pi^0)/BR(\pi^0\gamma\gamma)$ is a factor of 1277, so the background from this channel is still significant. The fraction of $\eta \rightarrow 3\pi^0$ events that leak into the 0.5-0.6 GeV mass range for $M(4\gamma)$ with a threshold of 0.1 GeV for FCAL showers is about 3.8×10^{-4} if both BCAL and FCAL are used and about 1.5×10^{-4} when all four photons are in the FCAL.

The production of $2\pi^0$ events presents another source of background whose reconstructed invariant mass can fall within the η mass window. The production of $\gamma p \rightarrow \pi^0\pi^0 p$ has been studied using different beam types and targets at low beam energies [72][73]. The production mechanism of $2\pi^0$ in our energy range is an important topic to be investigated. The kinematical features of $\gamma p \rightarrow \pi^0\pi^0 p$ production will be measured prior to the $\eta \rightarrow \pi^0\gamma\gamma$ analysis. The contribution from this channel is expected to be a smooth background that does not produce a peak in the η mass region. We studied $\gamma p \rightarrow \pi^0\pi^0 p$ background using a version of the Pythia event generator [74] modified for photo-production that incorporates

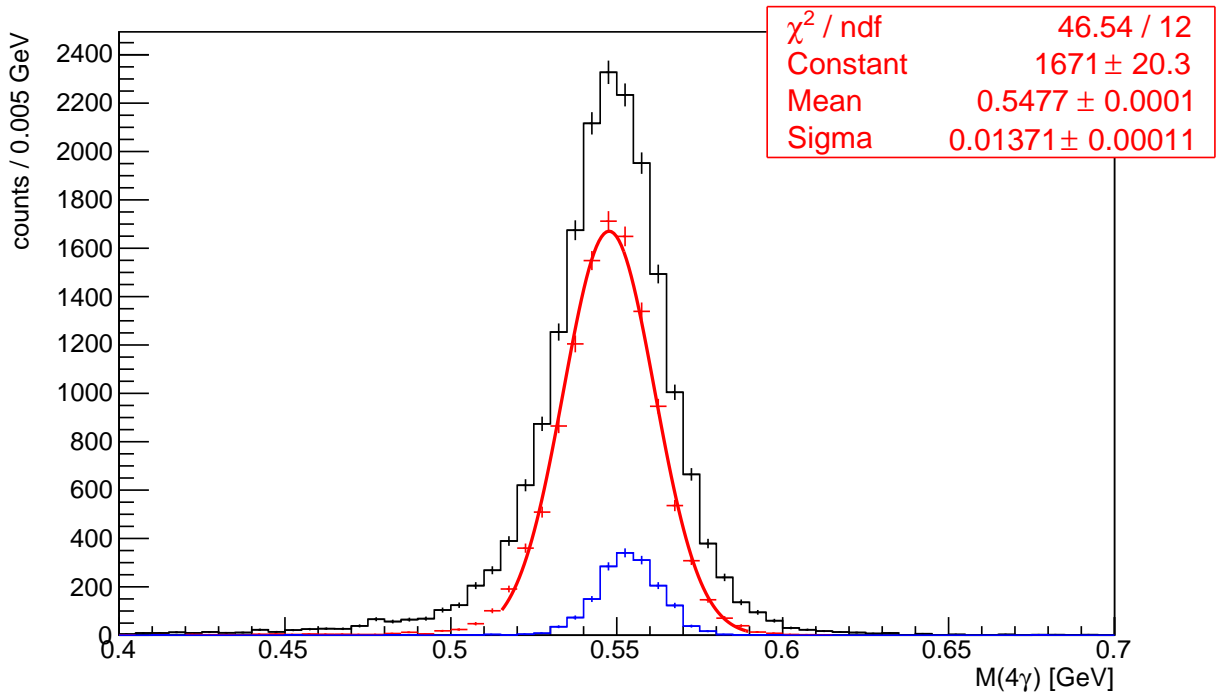


FIG. 9: Four-photon mass as a function of the calorimeter regions used to detect the photons using the measured four-vector quantities: (black) BCAL+FCAL, (red) FCAL (including insert), (blue) insert only. The threshold in the FCAL was 0.1 GeV.

both non-resonant production of the two-pion pairs and production through resonances such as $\gamma + p \rightarrow \pi^0 + \Delta^+ \rightarrow 2\pi^0 + p$; we are also pursuing an alternate model (described in Appendix A) based on exchanges of Reggeons. In addition, we also identified a set of other potential backgrounds originating from multiple photon final states such as $p 4\pi^0$, $p 3\pi^0\gamma$, $p 2\pi^0\gamma$, $p 2\pi^0\gamma\gamma$, $p 2\pi^0 K_L$, and $p \pi^0\gamma$. Background decay channels were selected from 1.8×10^{10} generated Pythia events. Events were passed through the detailed GlueX Geant simulation and were reconstructed using an Island reconstruction algorithm (see Appendix D in [1] for a brief description).

The 4γ invariant mass distributions for the $\eta \rightarrow \pi^0\gamma\gamma$ signal, $\eta \rightarrow 3\pi^0$ background, and the other hadronic backgrounds estimated using the Pythia event generator are shown in Fig. 12 for several different numbers of photons required to be detected in the insert. The statistics are normalized to one day of data taking with the GlueX detector operated at high-luminosity, corresponding to a photon flux of about 5×10^7 tagged photons per second

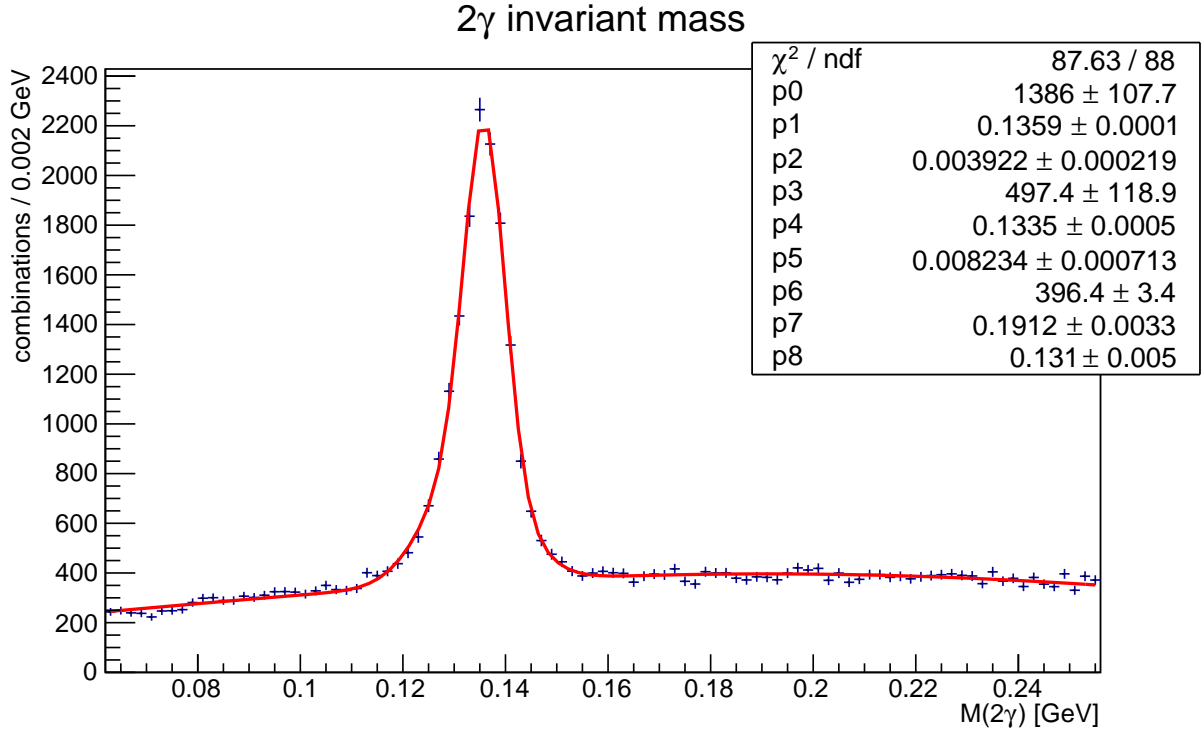
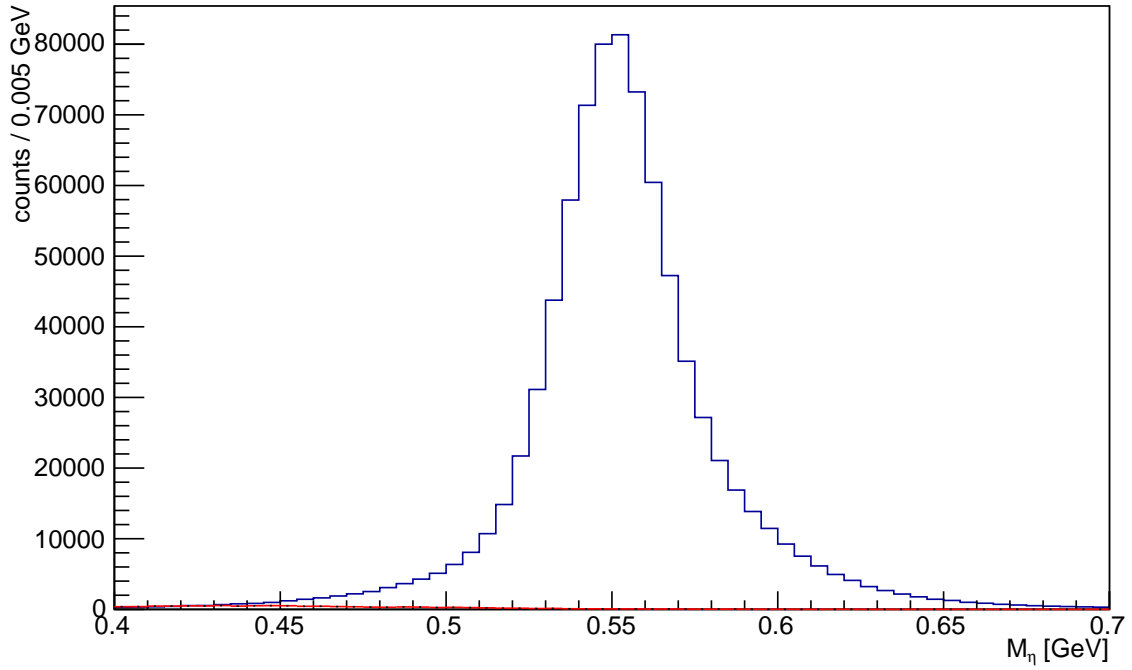


FIG. 10: Two-photon reconstruction showing the π^0 peak for an FCAL threshold of 0.1 GeV. The parameter p2 is the Gaussian σ of the core of the peak.

Condition	Efficiency	
	$E_{FCAL} > 0.1 \text{ GeV}$	$E_{FCAL} > 0.5 \text{ GeV}$
FCAL+BCAL	0.282	0.220
FCAL only	0.181	0.133
FCAL only, 2-4 γ 's in insert	0.172	0.128
FCAL only, 3-4 γ 's in insert	0.116	0.093
Insert only	0.025	0.022

TABLE IV: Reconstruction efficiencies for $\eta \rightarrow \pi^0 \gamma \gamma$ for various conditions. The incident photon energy range for events used in the analysis was 8-12 GeV.

in the coherent peak ($E_{beam} = 8.4 - 9 \text{ GeV}$). The η mesons were reconstructed in the beam energy range between 8.4 and 11.7 GeV. The FCAL threshold was 0.5 GeV. We required the missing energy to satisfy $|\Delta E| < 0.4 \text{ GeV}$ and $|\phi_{4\gamma} - \phi_p - 180^\circ| < 4^\circ$. The signal-to-background ratio estimates for various numbers of photons required to be detected in



$M(6\gamma)$

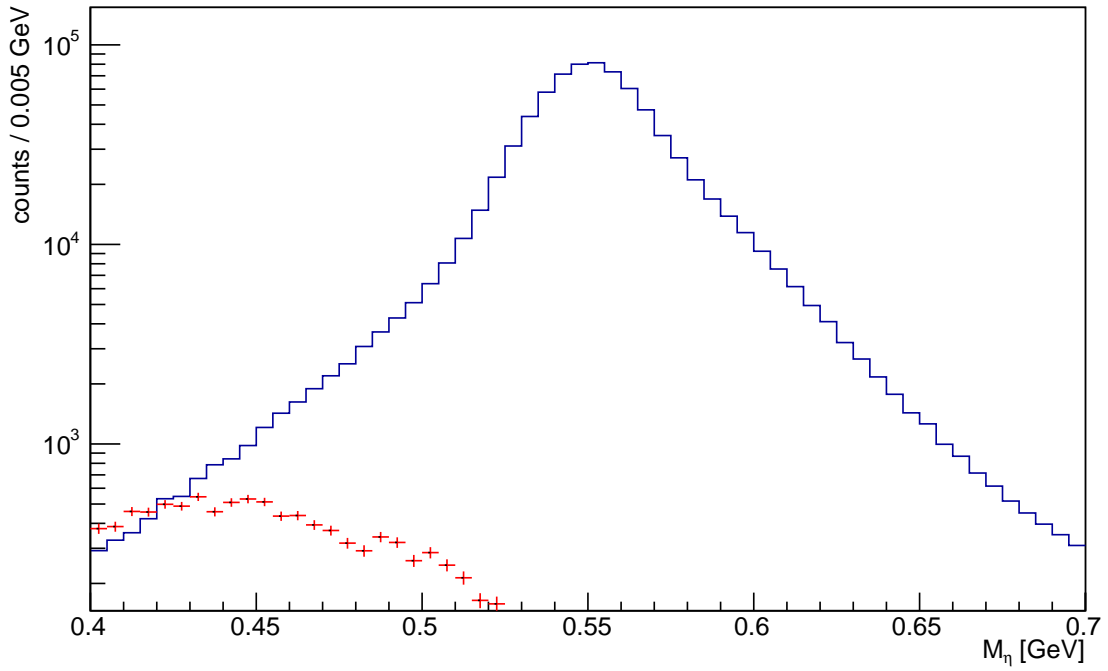


FIG. 11: Comparison between reconstructed 6γ mass (dark blue) from $\eta \rightarrow 3\pi^0$ using the measured four-vector quantities and the leakage into the 4γ channel (red). (top) linear scale; (bottom) log scale.

Condition	S/B
1-4 γ 's in insert	1.8
2-4 γ 's in insert	1.9
3-4 γ 's in insert	2.3
All γ 's in insert	3.9

TABLE V: Signal-to-background ratios for various numbers of photons required to be in the insert

the insert are shown in Table V; the expected signal-to-background ratio for events with at least three photons reconstructed in the lead tungstate insert (the best compromise between efficiency and background suppression) is about $S/B = 2.3$. In our original proposal [1], we estimated $S/B \sim 3$ for a stand-alone experiment with no DIRC in front of the FCAL and $E_{beam} > 9$ GeV and the four-photon efficiency we used in our $\eta \rightarrow \pi^0 \gamma \gamma$ rate estimate was 18.4%. The yield of reconstructed $\eta \rightarrow \pi^0 \gamma \gamma$ decays for our updated proposal is similar to that listed in the PAC42 proposal [1] by including counts from the coherent peak.

X. RATES UNDER THE GLUEX-IV RUNNING CONFIGURATION

A. Tagger coincidental rates

As shown in Fig 7, the Full Width Half Maximum (FWHM) for the reconstructed missing energy ($\Delta E = E_\gamma + m_p - E_\eta - E_{p'}$) for the $\gamma + p \rightarrow \eta + p$ reaction is about 350 MeV. If two hits in the tagger with an energy separation more than 350 MeV, it is possible to distinguish which photon is the right one for a physical event. Assuming the probability of hits follows the Poisson distribution, we define the coincidental rate for the photons in tagger as the probability ratio between the multi-hit events and the single-hit events in the photon tagger:

$$\frac{P(N > 1)}{P(N = 1)} = \frac{1 - (1 + n) \exp(-n)}{n \exp(-n)}, \quad (2)$$

where n is the average number of hits in the tagger per beam bunch crossing (4ns) per 350 MeV energy window. The Table VI summarize the photon rates and photon beam coincidental rates. As one can see, the photon beam coincidental rate is 17% for the coherent

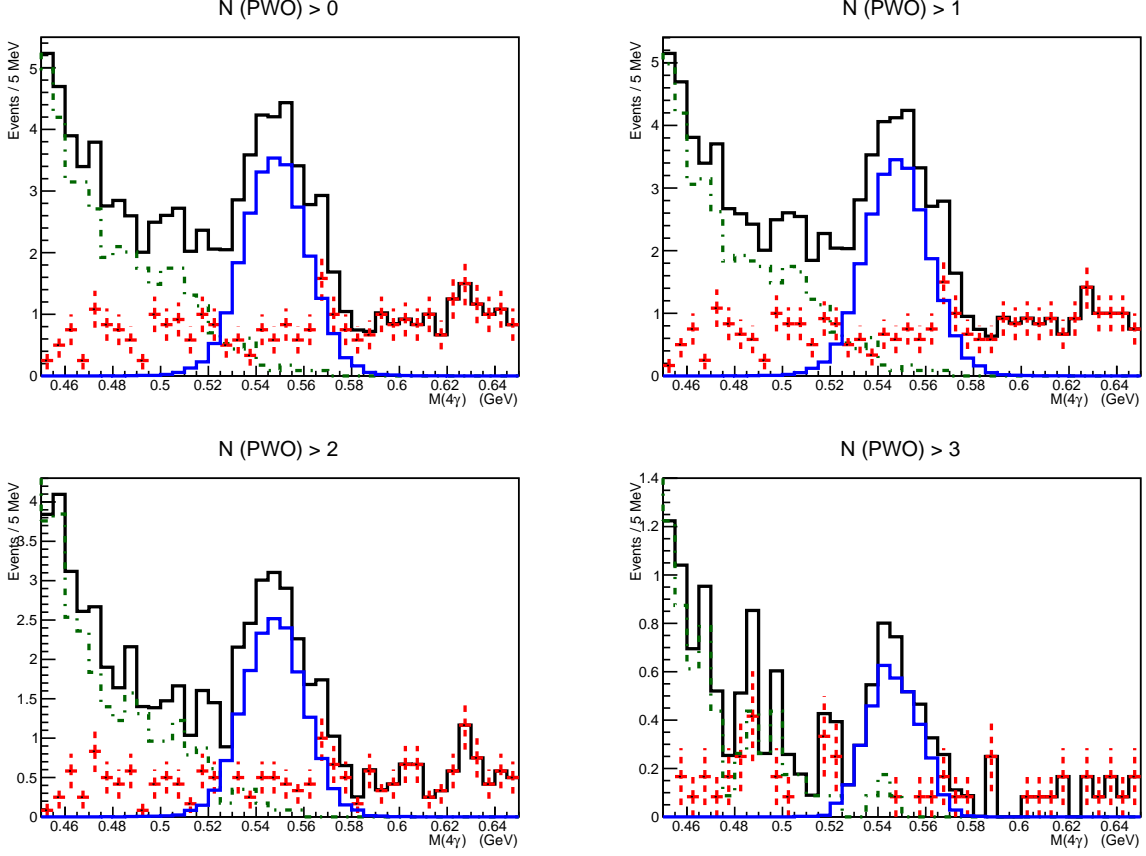


FIG. 12: Four photon invariant mass distributions for the signal $\eta \rightarrow \pi^0\gamma\gamma$ events (blue solid curves), $\eta \rightarrow 3\pi^0$ background (dash-dotted curves), and other hadronic backgrounds predicted by PYTHIA (red dashed curves). The black solid curves correspond to the sum of the signal and backgrounds. All yields are normalized to 1 day of taking data with GlueX at high luminosity. (top left) $N_\gamma(\text{insert}) > 0$; (top right) $N_\gamma(\text{insert}) > 1$; (bottom left) $N_\gamma(\text{insert}) > 2$; (bottom right) $N_\gamma(\text{insert}) > 3$.

peak ($E_\gamma = 8.4\text{--}9.0$ GeV) and is 7.3% above the coherent peak ($E_\gamma = 9.0\text{--}11.7$ GeV). The backgrounds due to mis-matching of the incident photon are manageable and can be subtracted by using out-of-time side bands for the data analysis. We will use the beam energy of 8.4–11.7 GeV for the $\eta^{(\prime)}$ decay measurement.

E_γ (GeV)	γ 's on tagger (Hz)	γ 's on target (Hz)	collimator acceptance (%)	coincidental rate (%)
8.4–9.0	1.3×10^8	5.1×10^7	41	17
9.0–11.7	2.7×10^8	4.3×10^7	16	7.3

TABLE VI: A summary for the photon rates on both tagger and target, and the photon coincidental rates in the tagger. The diameter of collimator is 3.4 mm.

B. Numbers of the tagged η and η'

The Hall D LH₂ target is 30 cm thick, or $N_p = 1.28 \times 10^{24}$ protons/cm². About 33% of these $\eta^{(\prime)}$'s are produced at too small an angle to allow a proton tag. The total rate of η/η' produced by the reaction $\gamma + p \rightarrow \eta^{(\prime)} + p$ with $\epsilon = 67\%$ proton detection is therefore calculated by

$$N_\eta = N_\gamma \cdot N_p \cdot \sigma \cdot \epsilon. \quad (3)$$

The expected numbers of the tagged mesons during GlueX-IV are shown in Table VII, which correspond to about $\sim 6.3 \times 10^7$ for η and $\sim 4.9 \times 10^7$ for η' per 100 days of beam time. As one can see, the production rates for η and η' are quite similar. The same data set will provide good statistics for both mesons.

	η	η'
Beam time (days)	200	200
σ ($E_\gamma \sim 8.4\text{--}9.0$)	98 (nb)	76 (nb)
σ ($E_\gamma \sim 9.0\text{--}11.7$)	80 (nb)	62 (nb)
Total tagged mesons	1.3×10^8	9.8×10^7

TABLE VII: The tagged η and η' for the approved GlueX-IV with 200 days of beam time. The average cross sections are calculated according to reference [71].

activities	Beam time (day)
LH ₂ production	100 days
Empty target and target-out runs	7 days
Tagger efficiency, TAC runs	3 days
FCAL-II commissioning, calibration, and checkout	12 days
Luminosity optimization (pile-up, accidentals studies)	8 days
Total	130 days

TABLE VIII: Beam time request in original JEF proposal [1].

XI. BEAM TIME

The average acceptance for our key signal channel $\eta \rightarrow \pi^0 \gamma \gamma$ is about a factor of 2 smaller than what was stated in the the original proposal [1] due to two reasons: (1) the size of the PWO crystal insertion in the current proposal is smaller compared to what was proposed in [1] and we will require at least three η decay photons detected by the PWO crystal part of calorimeter for signal reconstruction; (2) the beam energy range is extended from 9–11.7 GeV (in [1]) to 8–11.7 GeV (in the current proposal) in order to include the coherent bremsstrahlung photon peak. On the other hand, the photon flux is doubled because of additional coherent photons. Therefore, the total signal production rate remains almost the same as in the original proposal.

Based on PAC recommendation, we demonstrated that the JEF experiment has full capabilities to run in parallel to the GlueX experiment. If GlueX is extended after 2023, we will run concurrently with GlueX without a separate beam request, but with an additional 12 days for FCAL-II commissioning, calibration, and checkout. On the other hand, if there is no more GlueX run after 2023, we will request the same number of beam days as stated in the original proposal [1] which is copied here in Table VIII.

XII. SUMMARY

The JEF experiment has full capability to run in parallel to GlueX with an upgraded FCAL-II. Under the GlueX-IV running conditions, the numbers of tagged meson are $\sim 6 \times 10^7$ for η and $\sim 5 \times 10^7$ for η' per 100 days of beam time. The availability of significantly boosted mesons in Hall D, in combination with our proposed lead tungstate upgrade to the forward calorimeter, will improve the signal to background ratio for rare $\eta^{(\prime)}$'s decays to neutral channels with 3-5 photons by up to 2 orders of magnitude. The possibility of continuous taking data in parallel with all experiments using a LH₂ target in Hall D offers the potential to accumulate a large data sample during the JLab 12 GeV era. This will represent a unique η and η' factory in the world with no competition in the rare neutral decay modes. This will allow us to address a broad range of important physics topics, from a precision test of low energy QCD, to a sensitive probe for a sub-GeV leptophobic dark B' boson and the C-violating, P-conserving new forces that extend our knowledge to the dark sector and explore new sources of CP violation needed to explain the matter/anti-matter asymmetry in the universe. The discovery of such new forces beyond SM would have far-ranging implications into our understanding of symmetry and dark matter.

In addition, a state-of-the-art, high resolution, high granularity, and radiation resistant calorimeter (FCAL-II) will greatly enhance the GlueX experiment and all other experiments in Hall D. Installation of FCAL-II will have minimal impact on the run schedule in Hall D.

-
- [1] L. Gan *et al.*, Jlab proposal “Eta Decays with Emphasis on Rare Neutral Modes: The JLab Eta Factory (JEF) Experiment”, https://www.jlab.org/exp_prog/proposals/14/PR12-14-004.pdf.
 - [2] C. Meyer, *et al.*, JLab proposal “An initial study of mesons and baryons containing strange quarks with GlueX”, https://www.jlab.org/exp_prog/proposals/13/PR12-13-003.pdf.
 - [3] M.J. Ramsey-Musolf, talk at workshop on “Hadronic Probes of Fundamental Symmetries”, the Amherst Center for Fundamental Interactions (ACFI), University of Massachusetts, Amherst, MA, March 6-8, 2014. <https://www.physics.umass.edu/acfi/seminars-and-workshops/hadronic-probes-of-fundamental-symmetries> .

- [4] J. Alexander et al., Dark Sector 2016 Workshop: Community Report, arXiv:1608.08632.
- [5] B.M.K. Nefkens and J.W. Price, Phys. Scr. **T99** , 114 (2002).
- [6] E.L. Bratkovskaya *et al.*, Phys. Lett. B **359**, 217 (1995).
- [7] J. Beringer *et al.*, (Particle Data Group), PRD 86, 010001 (2012).
- [8] S. Tulin, H. Yu, K.M. Zurek, Phys. Rev. Lett. **110**, 111301 (2013).
- [9] S. Tulin, H. Yu, K.M. Zurek, Phys. Rev. D **87**, 115007-1 (2013).
- [10] J. F. Navarro, C. S. Frenk, and S. D. M. White, Astrophys. J. **490**, 493 (1997).
- [11] R. H. Wechsler, J. S. Bullock, J. R. Primack, A. V. Kravtsov, and A. Dekel, Astrophys. J. **568**, 52 (2002).
- [12] J. Dubinski and R. G. Carlberg, Astrophys. J. **378**, 496 (1991).
- [13] R. A. Flores and J. R. Primack, Astrophys. J. **427**,L1 (1994).
- [14] J. D. Simon, A. D. Bolatto, A. Leroy, L. Blitz, and E. L. Gates, Astrophys. J. **621**, 757 (2005).
- [15] R. K. de Naray and K. Spekkens, Astrophys. J. **741**, L29 (2011).
- [16] W. J. G. de Blok, S. S. McGaugh, A. Bosma, and V. C. Rubin, Astrophys. J. **552**, L23 (2001).
- [17] M. Boylan-Kolchin, J. S. Bullock, and M. Kaplinghat, Mon. Not. R. Astron. Soc. **415**, L40 (2011).
- [18] M. Boylan-Kolchin, J. S. Bullock, and M. Kaplinghat, Mon. Not. R. Astron. Soc. **422**, 1203 (2012).
- [19] L. E. Strigari, J. S. Bullock, M. Kaplinghat, J. Diemand, M. Kuhlen, and P. Madau, Astrophys. J. **669**, 676 (2007).
- [20] P. Langacker, Rev. Mod. Phys. **81**, 1199 (2009).
- [21] G.R. Farrar and G. Zaharijas, Phys. Rev. Lett. **96**, 041302 (2006).
- [22] M. Duerr and P.F. Perez, Phys. Lett. B **732**, 101 (2014).
- [23] H. Davoudiasl *et al.*, Phys. Rev. Lett. **105**, 211304 (2010)
- [24] K. Agashe and G. Servant, Phys. Rev. Lett. **93**, 231805 (2004)
- [25] M.L. Graesser, I.M. Shoemaker, L. Vecchi, arXiv:1107.2666.
- [26] B. Batell *et al.*, Phys. Rev. D **90**, 115014 (2014).
- [27] B. Holdom, Phys. Lett. B **166**, 196 (1986).
- [28] R. Essig *et al.*, arXiv:1311.0029.
- [29] S. Abrahamyan et al. (APEX), Phys. Rev. Lett. **107**, 191804 (2011), 1108.2750.
- [30] M. Battaglieri et al., Nucl. Instrum. Meth. A777, **91** (2015), 1406.6115.

- [31] J. Balewski et al. (2014), arXiv:1412.4717.
- [32] M. Battaglieri et al., (2016), arXiv:1607.01390.
- [33] A. E. Nelson and N. Tetradis, Phys. Lett. B **221**, 80 (1989).
- [34] S. Tulin, Phys. Rev. D **89**, 114008 (2014).
- [35] T.D. Lee and C.N. Yang, Phys. Rev. **98**, 1501 (1955).
- [36] R. Foot, G. C. Joshi, and H. Lew, Phys. Rev. D **40**, 2487 (1989).
- [37] S. Rajpoot, Phys. Rev. D **40**, 2421 (1989); X.-G. He and S. Rajpoot, Phys. Rev. D **41**, 1636 (1990); C. D. Carone and H. Murayama, Phys. Rev. Lett. **74**, 3122 (1995); D. C. Bailey and S. Davidson, Phys. Lett. B **348**, 185 (1995); C. D. Carone and H. Murayama, Phys. Rev. D **52**, 484 (1995); A. Aranda and C. D. Carone, Phys. Lett. B **443**, 352 (1998); P. Fileviez Perez and M. B. Wise, Phys. Rev. D **82**, 011901 (2010).
- [38] B. Dobrescu and C. Frugiuele, Phys. Rev. Lett. **113**, 061801 (2014).
- [39] T. Cohen *et al.*, Phys. Rev. Lett. **115**, 171804 (2015).
- [40] H. Davoudiasl and R.N. Mohapatra, New J. Phys. **14**, 095011 (2012); K.M. Zurek, Phys. Rept. **537**, 91 (2014); K. Petraki and R.R. Volkas, Int. J. Mod. Phys. A **28**, 1330028 (2013).
- [41] M. Williams, C. Burgess, A. Maharana, and F. Quevedo, JHEP **1108**, 106 (2011).
- [42] A. Aranda and C. D. Carone, Phys. Lett. B **443**, 352 (1998).
- [43] R. Barbieri and T. E. O. Ericson, Phys. Lett. B **57**, 270 (1975).
- [44] D. Babusci *et al.*, Phys. Lett. B **720**, 111 (2013).
- [45] P. Adlarson *et al.*, Phys. Lett. B **726**, 187 (2013).
- [46] B.A. Dobrescu and C. Frugiuele, JHEP **02**, 019 (2015).
- [47] E. Won et al. (Belle Collaboration), Phys. Rev. D **94**, 092006 (2016).
- [48] S. Fang, PoS CD15, 032 (2015).
- [49] S. Giovannella, PoS CD15, 035 (2015).
- [50] F. Ambrosino, et al., PoS CD09 (2009) 045.
- [51] E.P. Solodov, et al., AIP Conf.Proc., **1735**, 020005 (2016).
- [52] V.M. Aulchenko, et al., Nucl.Phys.Suppl., **376**, 181 (2008).
- [53] Yu.M. Shatunov, et al., Proc. Of the 7th European Particle Accelerator, Vienna, Austria, 439 (2000).
- [54] A. Abashian, et al., Nucl.Instrum.Meth., **A 479**, 117 (2002).
- [55] B. Aubert, et al., Nucl.Instrum.Meth., **A 479**, 1 (2002).

- [56] T. Konno, J.Phys.:Conf.Ser., **627**, 012009 (2015).
- [57] S. Prakhov, et al.,Phys.Rev., **C 79**, 035204 (2009); E.F. McNicoll, et al.,Phys.Rev. , **C 82**, 035208 (2010).
- [58] R. Maier, Nucl.Instrum.Meth., **A 390**, 1 (1997).
- [59] H.H. Adam, et al., arXiv:nucl-ex/0411038.
- [60] N. H'usken, et al., EPJ Web Conf., bf 113, 05023 (2016).
- [61] A. Goswami, et al., Proc. Of the DAE-BRNS Symp. on Nucl. Phys., **60**, 692 (2015).
- [62] R. Arnaldi, et al. (NA60 collaboration), Phys.Lett. **B 757**, 437 (2016).
- [63] A. Aaij, et al.,Phys.Lett., **B 764**, 233 (2017).
- [64] E. Ramberg, talk at APS April meeting, Jan 28-31, 2017, Washington DC.
- [65] S. Tulin, private communication.
- [66] M. Pospelov, A. Ritz and M. Voloshin, Phys. Rev. D **78**, 115012 (2008).
- [67] C. Fanelli and M. Williams, J.Phys., G **44(1)**, 014002 (2016).
- [68] C. Patrignani, et al. (Particle Data Group), Chin. Phys. C **40**, 100001 (2016).
- [69] R. Escribano, PoS QNP **2012**, 079 (2012) [arXiv:1207.5400 [hep-ph]].
- [70] F. K. Guo, B. Kubis and A. Wirzba, Phys. Rev. D **85**, 014014 (2012) doi:10.1103/PhysRevD.85.014014 [arXiv:1111.5949 [hep-ph]].
- [71] J. M. Laget, Phys. Rev. C **72** (2005) 022202 [hep-ph/0502233].
- [72] S. Prakhov *et al.*, Phys. Rev., **C69**, 042202 (2004).
- [73] T. Matsumura *et al.*, Nucl. Phys., **A721**, 723 (2003).
- [74] <http://home.thep.lu.se/~torbjorn/Pythia.html>; we are using version 6.
- [75] A. Donnachie and Y. S. Kalashnikova, arXiv:0806.3698 [hep-ph]; A. Donnachie and Y. S. Kalashnikova, Phys. Rev. C **93**, no. 2, 025203 (2016) [arXiv:1507.07408 [hep-ph]].
- [76] J. J. Xie and E. Oset, Eur. Phys. J. A **51**, 111 (2015) [arXiv:1412.3234 [nucl-th]].

APPENDIX A: ALTERNATE $2\pi^0$ MODEL

The production of double π^0 events presents a significant source of background to the rare decay $\eta \rightarrow \pi^0\gamma\gamma$ that can in principle be suppressed with a suitable cut to veto a second π^0 in the event. Analysis of the recent GlueX data taken in spring 2016 indicates substantial

weight in the two- π^0 mass spectrum below the $f_0(980)$, as shown in Fig. 13. An event gen-

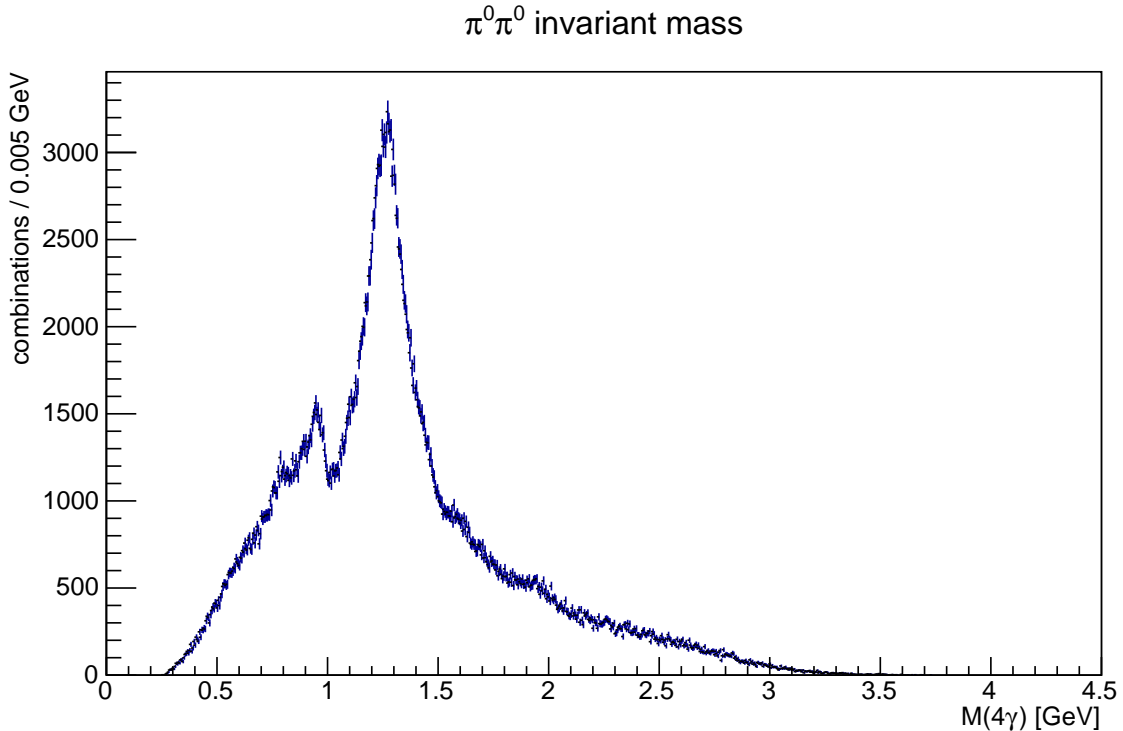


FIG. 13: Mass distribution of $\pi^0\pi^0$ events taken from the spring 2016 GlueX data set. The beam energy range was 3-11.8 GeV.

erator was developed for the production of scalar mesons based on the model by Donnachie and Kalashnikova [75] for $f_0(980)$ production. The low mass enhancement was assumed to be due to the $f_0(500)$, which was modeled in the same manner as the $f_0(980)$. The enhancement near 1.27 GeV in the measured spectrum is mostly due to the $f_2(1270)$. This was added to the generator following the model of Xie and Oset [76]. Destructive interference between the $f_0(980)$ and the other waves produces the dip in the measured distribution between the $f_0(980)$ mass region and the $f_2(1270)$; this interference is incorporated into the event generator. Fig. 14 shows an example of the mass distribution produced by the generator. After the acceptance of the detector is taken into account, the distribution agrees reasonably well with the data (Fig. 13).

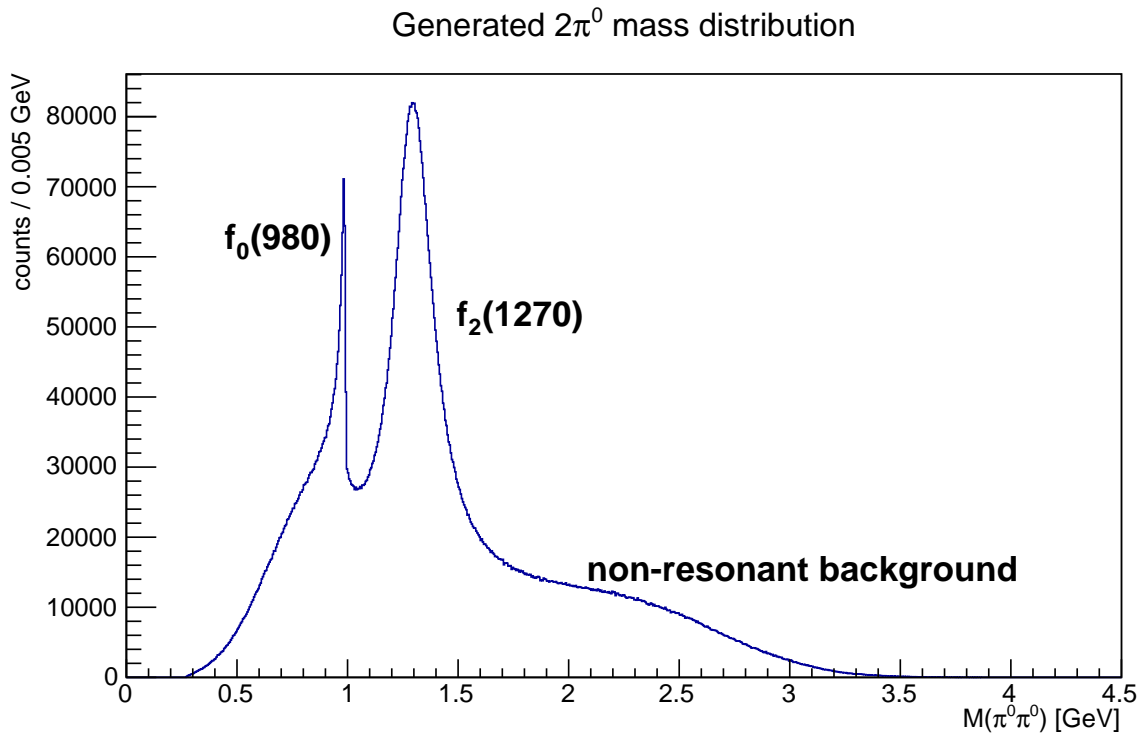


FIG. 14: (top) Generated $\pi^0\pi^0$ distribution. (bottom) Accepted distribution.